Science of the Total Environment 615 (2018) 857–874

Contents lists available at ScienceDirect

Science of the Total Environment

journal homepage: www.elsevier.com/locate/scitotenv

Review

Potential for using remote sensing to estimate carbon fluxes across northern peatlands – A review

Lees K.J. [a,*], Quaife T. [b], Artz R.R.E. [c], Khomik M. [c], Clark J.M. [a]

[a] Department of Geography and Environmental Science, University of Reading, Whiteknights, PO box 227, Reading RG6 6AB, UK
[b] Department of Meteorology, University of Reading, Earley Gate, PO box 243, Reading RG6 6BB, UK
[c] The James Hutton Institute, Craigiebuckler, Aberdeen AB15 8QH, UK

HIGHLIGHTS

- Optical data can be used to drive models of peatland carbon flux.
- Water, temperature and vegetation indices are important model factors.
- Challenges from peatland heterogeneity and vegetation composition
- Remote sensing driven models have the potential to fill gaps in current research

GRAPHICAL ABSTRACT

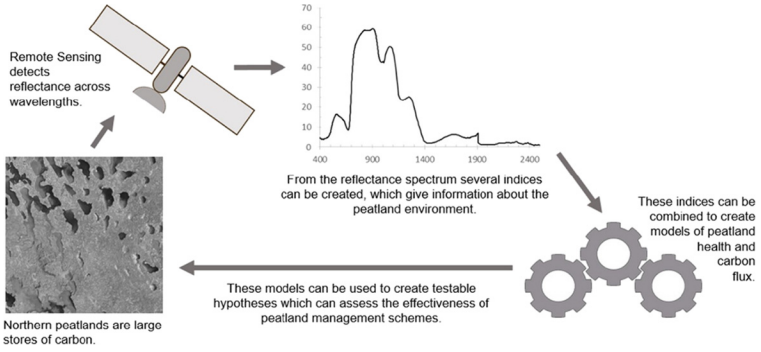

ARTICLE INFO

Article history:
Received 5 May 2017
Received in revised form 8 September 2017
Accepted 11 September 2017
Available online xxxx

Editor: Simon Pollard

ABSTRACT

Peatlands store large amounts of terrestrial carbon and any changes to their carbon balance could cause large changes in the greenhouse gas (GHG) balance of the Earth's atmosphere. There is still much uncertainty about how the GHG dynamics of peatlands are affected by climate and land use change. Current field-based methods of estimating annual carbon exchange between peatlands and the atmosphere include flux chambers and eddy covariance towers. However, remote sensing has several advantages over these traditional approaches in terms of cost, spatial coverage and accessibility to remote locations. In this paper, we outline the basic principles of using remote sensing to estimate ecosystem carbon fluxes and explain the range of satellite data available for

Abbreviations: μm, micrometer (10^{-6}); APAR, Absorbed Photosynthetically Active Radiation; AVHRR, Advanced Very High Resolution Radiometer; CAI, Cloud and Aerosol Imager; CH_4, Methane; CO_2, Carbon dioxide; DIC, Dissolved Inorganic Carbon; DOC, Dissolved Organic Carbon; DoD, Department of Defence; EC, Eddy Covariance; EF, Evaporative Fraction; EO, Earth Observation; EOM, Ecosystem Organic Matter; ESA, European Space Agency; ETM+, Enhanced Thematic Mapper Plus; EUMETSAT, European Organization for the Exploration of Meteorological Satellites; EVI, Enhanced Vegetation Index; fBWI, floating Water Band Index; FIR, Far-Infrared; FTS, Fourier Transform Spectrometer; GHG, Greenhouse Gas; GLO-PEM, Global Production Efficiency Model; GMAO, Global Modelling and Assimilation Office; GOSAT, The Greenhouse Gases Observing Satellite; GPP, Gross Primary Productivity; H_2O, water; InSAR, Interferometric Synthetic Aperture Radar; IR, Infra-Red; IRGA, Infra-Red Gas Analyser; JAXA, Japan's Aerospace Exploration Agency; LAI, Leaf Area Index; LiDAR, Light Detection and Ranging; LST, Land Surface Temperature; LSWI, Land Surface Water Index; LUE, Light Use Efficiency; MERIS, Medium Resolution Imaging Spectrometer; MIR, Mid-Infrared; MODIS, Moderate Resolution Imaging Spectrometer; MSI, Multi-Spectral Imager; MTCI, MERIS Terrestrial Chlorophyll Index; NASA, National Aeronautics and Space Administration; NDVI, Normalised Difference Vegetation Index; NDWI, Normalised Difference Water Index; NEE, Net Ecosystem Exchange; nm, nanometer (10^{-9}); O_2, Oxygen; OCO, Orbiting Carbon Observatory; OLI, Operational Land Imager; PAR, Photosynthetically Active Radiation; POC, Particulate Organic Carbon; PRI, Photosynthetic Reflectance Index; Ra, autotrophic Respiration; R_{eco}, ecosystem Respiration; REP, Red Edge Position; Rg, growth Respiration; Rh, heterotrophic Respiration; Rm, maintenance Respiration; RS, Remote Sensing; RSPB, Royal Society for the Protection of Birds; SAR, Synthetic Aperture Radar; SIF, Solar Induced Fluorescence; SLSTR, Sea and Land Surface Temperature Radiometer; SOM, Soil Organic Matter; SPOT, Satellite Pour l'Observation de la Terre; Suomi-NPP, Suomi National Polar Orbiting Partnership; SWIR, Short-Wave Infrared; TANSO, Thermal and Near-infrared Sensor for carbon Observation; TIR, Thermal Infra-Red; USGS, United States Geological Survey; VI, Vegetation Index; VIIRS, Visible Infrared Imaging Radiometer Suite; VPM, Vegetation Photosynthesis Model; VPD, Vapour Pressure Deficit; WI, Water Index; WTD, Water Table Depth.

* Corresponding author.
E-mail address: K.J.Lees@pgr.reading.ac.uk (K.J. Lees).

https://doi.org/10.1016/j.scitotenv.2017.09.103

Keywords:
Satellites
GPP
Respiration
NEE
Vegetation indices
Restored peatlands

such estimations, considering the indices and models developed to make use of the data. Past studies, which have used remote sensing data in comparison with ground-based calculations of carbon fluxes over Northern peatland landscapes, are discussed, as well as the challenges of working with remote sensing on peatlands. Finally, we suggest areas in need of future work on this topic. We conclude that the application of remote sensing to models of carbon fluxes is a viable research method over Northern peatlands but further work is needed to develop more comprehensive carbon cycle models and to improve the long-term reliability of models, particularly on peatland sites undergoing restoration.

Contents

1. Introduction

Peatlands are a large store of terrestrial carbon and any change in their carbon balance could therefore cause large changes in the atmospheric greenhouse gases (GHGs) of the planet. The atmospheric store of carbon is estimated to be about 750 Gt C, compared to an estimated 500 ± 100 Gt C stored in Northern peatlands (Yu, 2012). Although peatlands are an important part of the terrestrial carbon cycle and store approximately a third of the world's soil carbon (Gorham, 1991; Limpens et al., 2008), there is still much uncertainty about how these areas are affected by climate and land use change. There is also much variation between peatland types, with the greatest difference between acidic rain-fed bogs and more nutrient rich minerotrophic fens. Peat bogs in pristine condition are considered to be net carbon sinks (Yu, 2012), yet many areas of peatland have experienced degradation through human activity (such as draining, grazing and burning and conversion to plantation forestry), which decreases the net carbon uptake from the atmosphere (Fleischer et al., 2016). Peatland restoration is recognised as one of the ways to reach carbon emission reduction targets under the Kyoto Protocol (Hiraishi et al., 2013; IPCC, 2014), and it is therefore essential to develop ways of verifying and quantifying the effect of such restoration procedures. Field measurement techniques are limited by scale and cost, whereas Remote Sensing (RS) presents an opportunity to provide data to carbon flux models over large areas quickly and cheaply.

Peatland ecosystems differ from other areas due to their high water table and very distinctive vegetation composition. Fluctuations in the water table influence the amount and distribution of oxygen available in the soil profile, which in turn influences carbon emissions. The carbon cycle of peatland ecosystems is complex and includes many components (a conceptual diagram of key components of the cycle in peat bogs is shown in Fig. 1). CO_2 enters the peatland system though photosynthesis of the vegetation (Gross Primary Productivity or GPP), and leaves it through autotrophic (plant) respiration (Ra), and heterotrophic respiration (Rh) (microbial decomposition). The sum of Ra and Rh gives ecosystem respiration (R_{eco}), whilst the difference between R_{eco} and GPP equals Net Ecosystem Exchange (NEE).

Models using RS data focus on estimating GPP, R_{eco} and also NPP – Net Primary Productivity, which is the difference between GPP and Ra. The various flux processes in the peatland carbon cycle are typically considered at timescales from hours to a few years, largely due to the short monitoring records currently available. Over the course of a peatland's lifetime which often spans several millennia, however, natural (e.g. natural fires) and human (e.g. afforestation) disturbances should also be considered to capture the full breadth of a peatland's carbon cycle, as should shifts in climatic conditions. Methane (CH_4) is not considered in this review, as methane and carbon dioxide are often studied separately and require different methodologies. At this time, RS methods for estimating CH_4 emissions are still in their infancy compared to those of CO_2 estimates (see Tagesson et al., 2013). In peatland, carbon can also leave the system as dissolved organic/inorganic carbon (DOC/DIC) in streams and pipe outflow, or as particulate organic carbon (POC) due to surface erosion through wind and washout; these are not included in RS estimations of NEE. For more information about the peatland carbon cycle see Limpens et al. (2008). The current review focuses on biogenic CO_2 fluxes, which are the largest and most variable component at annual timescales (Helfter et al., 2015).

Field based studies show that several factors affect the spatial and temporal variance of carbon fluxes across peatlands, particularly water table depth (WTD) and temperature (Lafleur et al., 2003; Bubier et al., 2003; Dinsmore et al., 2009; Lund et al., 2012; Strachan et al., 2016). Temperature and WTD help to determine plant species composition in the long term, while, in the shorter term, changes in these climatic variables affect plant photosynthesis and soil respiration (Bubier et al., 2003). Unusually dry or drained peatlands produce more CO_2 but less CH_4, whilst in wet peatlands this is reversed (Waddington and Price, 2000).

Peatland NEE is also strongly linked to vegetation composition, as different plant species have differing responses to climatic variables, and provide differing quantities of available organic matter for microbial

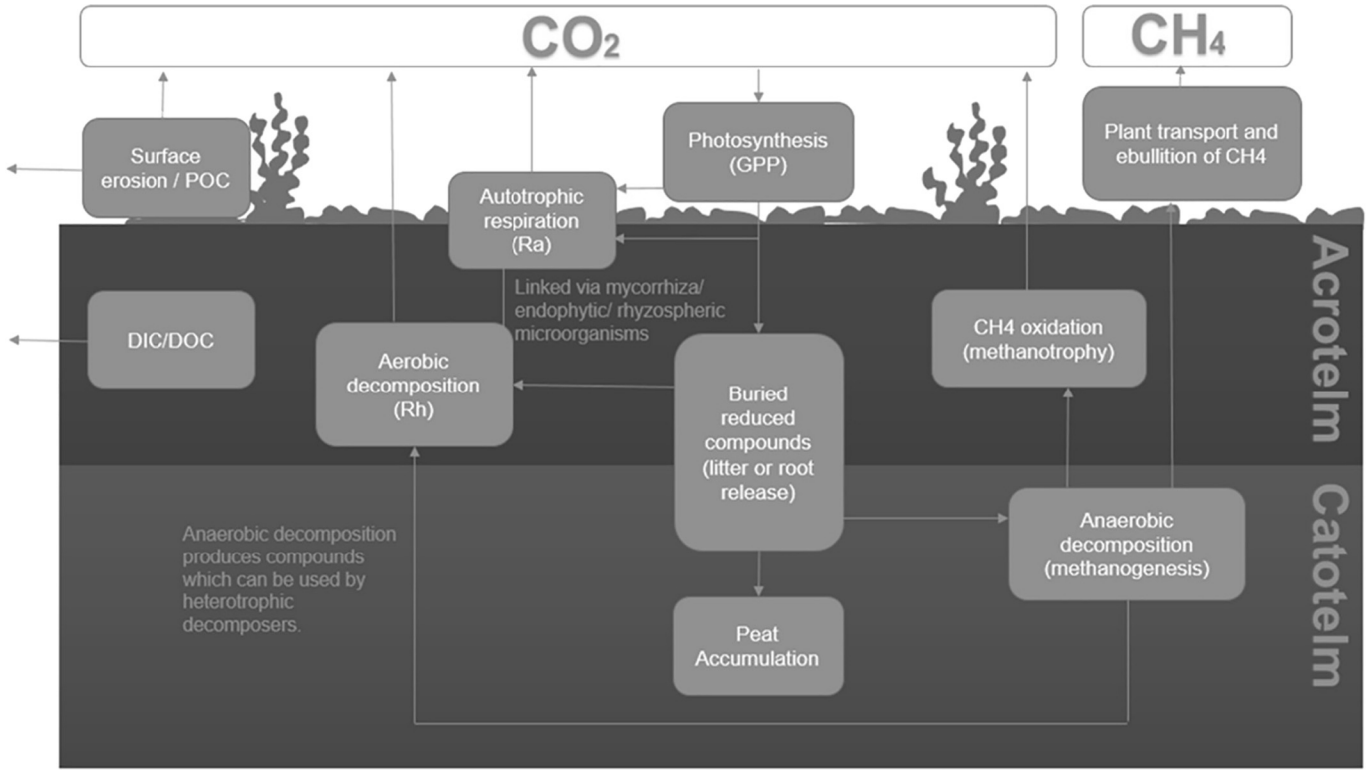

Fig. 1. Simplified carbon cycle in peat bogs. The catotelm is deep peat which remains saturated, whilst the acrotelm is where the water table varies. Net Ecosystem Exchange (NEE) is the combination of Gross Primary Productivity (GPP) and all ecosystem Respiration (R_{eco}). R_{eco} is the combination of autotrophic respiration (Ra) and aerobic decomposition/heterotrophic respiration (Rh). Net Primary Productivity (NPP) is the combination of GPP and Ra.

decomposition. Different vegetation species dominate on different peatland types, with the most commonly considered distinction being between bog and fen. Bogs are generally acidic and support *Sphagnum* moss cover, whilst fens are more variable and support a greater proportion of sedges. The composition of vegetation communities is also affected by the site's microtopography, which often consists of areas of low waterlogged land (hollows), lawns, and higher, dryer areas (hummocks) (Lindsay et al., 1985; Nilsson et al., 2008) (see Fig. 2). This paper considers variations in peatland topography at the microscale (hummocks and hollows, 0.2 to 2 m), mesoscale (pools and intrusions of forest etc. 2 to 50 m), and macroscale (landscape level).

Current field-based methods of estimating NEE on peatlands include flux chambers and eddy covariance (EC) towers (see Fig. 3). Chamber studies measure NEE on a cm^2 scale, and so are useful for gaining information about microscale spatial heterogeneity of fluxes within peatland sites, such as contributions of different species and microtopographic variations. However, due to logistical constraints, chamber measurements are often taken infrequently and over relatively brief timescales, so temporal variation is poorly explored (Marushchak et al., 2013). Furthermore, the small spatial scale does not allow for easy upscaling due to the difficulty of averaging or interpolating across such a varied landscape (Humphreys et al., 2006). EC towers estimate NEE over a larger area (m^2 to km^2), known as a footprint, from measurements of CO_2 concentration and air turbulence. Flux tower measurements are recorded at high frequency and over relatively extended periods of time (i.e. able to record half-hourly averages of CO_2 measurements taken at frequencies of around 10 Hz all year round), allowing good analysis of temporal variation over the site. However, EC towers have high equipment and maintenance costs, often suffer down-time due to equipment failure, and there are not many in place on peatland sites. The data from EC towers are also often noisy and prone to gaps. The spatial heterogeneity of peatlands means that a single flux tower cannot necessarily be assumed to be a good proxy for an entire landscape or region.

Remote sensing has several advantages over traditional field studies, in particular, cost, scale, and viewing of remote locations. While RS also includes measurements by aeroplanes, unmanned aerial vehicles and kites, here we focus exclusively on satellite remote sensing. Satellites such as Terra, Aqua and Landsat have been used in many studies of terrestrial carbon fluxes over various ecosystems (Prince and Goward, 1995; Xiao et al., 2004; Yuan et al., 2010; Sims et al., 2008; Wu, 2012). Many satellite datasets are freely available, have a regular resampling interval (between one and sixteen days for the most widely used satellites) and cover large areas of land (Harris et al., 2005; Crichton et al., 2014). Some also have a relatively long time series archive (e.g. Landsat, dating from the 1970s). Remote sensing also has the advantage of allowing researchers to be able to study an environment whilst minimising exposure to the risks of field work, and disruption to the environment in question, as well as maximising the usefulness of available resources (Malenovsky et al., 2015). It has the potential to be particularly useful for peatland studies, which often cover large isolated areas and can be difficult to access for continuous field studies (Connolly et al., 2009). However, data from many satellites have a coarse spatial resolution which makes it difficult to accurately distinguish the small scale heterogeneity of peatlands (Crichton et al., 2014). Remote sensing in general is limited by the fact that it only measures energy incident at the sensor, the distribution of which (e.g. as a function of wavelength) then has to be used to infer the characteristics of interest. Such techniques cannot measure gas fluxes directly and rely on models to estimate properties such as GPP and NEE. The extreme remoteness of satellite data also means that the radiation is affected by absorption by gases in the atmosphere, and atmospheric scattering from aerosols and other molecules, which can reduce its accuracy (Vermote et al., 1997). Peat bog areas are particularly prone to heavy rainfall and therefore cloud cover due to their prevalence in, and indeed reliance upon, humid environments.

Despite recent advances in the use of remote sensing to monitor carbon fluxes across ecosystems such as forests and cropland (e.g. Xiao

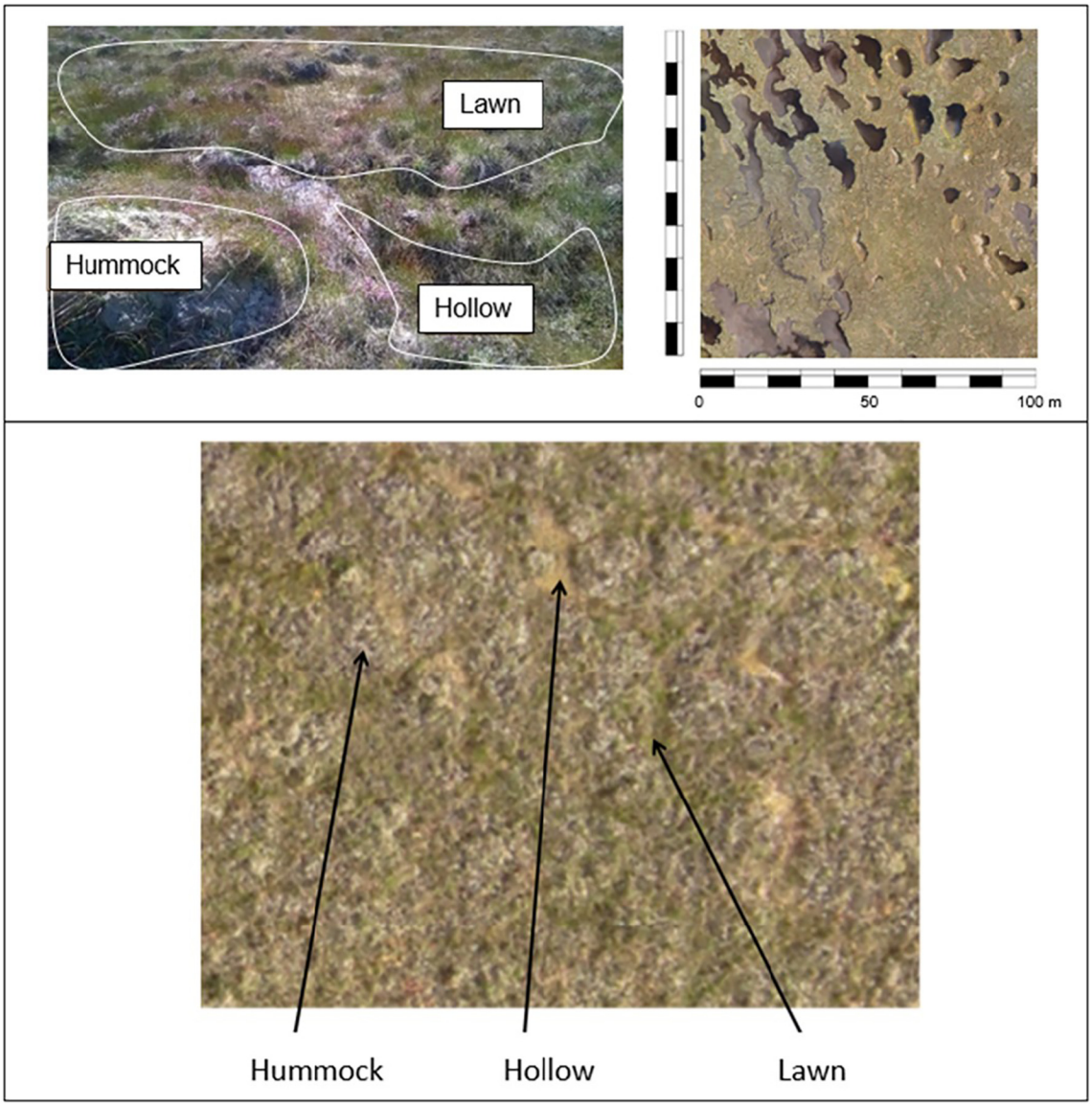

Fig. 2. Photo showing peatland microtopography at Forsinard Flows RSPB reserve, Scotland. Hummocks are raised features, hollows are depressed, and lawns are relatively flat surfaces. Each of these features is also characterised by a different vegetation complement. Top left: View as seen by the human eye. Top right: a 100 m^2 area as the satellite would see it (5 cm resolution aerial photography). Lower image: The microtopographical features across an area of 10 m by 8 m using 5 cm resolution aerial photography.

et al., 2004; Sims et al., 2008; Yuan et al., 2010), less attention has been given to the application of RS in peatland areas even though they are a critical component of the carbon cycle (Yu, 2012). In this review paper we evaluate the current state of knowledge concerning the estimation of CO_2 fluxes in peatland using remote sensing and identify priority areas in need of future research. This review paper consists of five sections including this introduction. Section 2 reviews current methodologies, summarizing key satellites used and various methods of estimation of peatland carbon dynamics from RS data. Several of the most commonly used models and their strengths and weaknesses are discussed. Section 3 reflects on previous studies where remote sensing was used to estimate carbon and water dynamics over peatlands. The insights gained in this section generate an assessment of those model parameters likely to produce the best results in a peatland landscape, and offer an understanding of current research gaps. Section 4 considers the challenges which the researcher must be aware of when using remote sensing to study peatlands, and suggests ways in which these difficulties may be overcome. The final discussion section (Section 5) summarises the areas of research in this topic which are at the forefront of current study and are only just beginning to be explored, as well as the main areas in need of further work concerning the estimation of CO_2 fluxes in peatlands using remote sensing.

2. Methods of measuring carbon fluxes remotely

2.1. Satellite sensors: what do they measure?

Some of the most commonly used remote sensing instruments are passive sensors detecting reflectance within the electromagnetic spectrum (see Fig. 4). This includes visible and near-infrared (NIR), and also thermal infrared (TIR) and microwave sensing spectroscopy. Visible and NIR sensors detect changes in the absorbance/reflectance ratio over landscapes. Where there is a large cover of green plants, for instance, green light will be reflected and red light absorbed, causing a peak in the green wavelengths detected by the sensor. Vegetation indices make use of this effect (see Section 2.2.2). Similarly, TIR spectroscopy can be used to measure surface temperatures and also to infer soil water content by detecting thermal infrared radiation emitted by a surface (Harris et al., 2006).

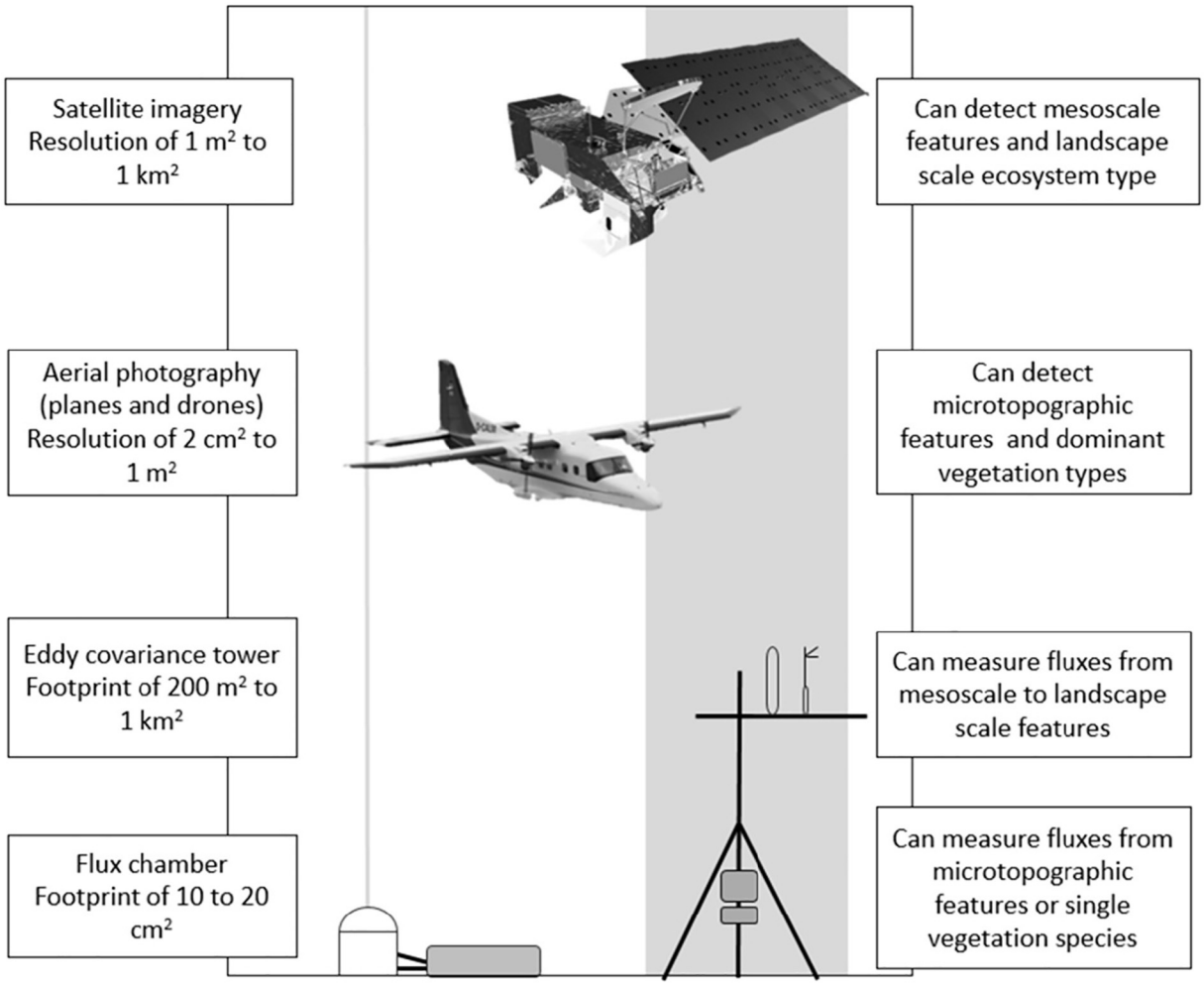

Fig. 3. Spatial scales at which carbon flux estimation tools can operate. The shading indicates a rough guide to the footprint of a flux chamber and an EC tower, compared to the footprint of a satellite such as MODIS (whole box). Aerial remote sensing is included here but not discussed in the text. Microscale is considered to be changes in topography and vegetation up to 2 m, whilst mesoscale concerns larger areas of variation, such as bog pools or small areas of forestry.
(Aeroplane image from NERC, 2016; satellite image from NASA, 2010).

Active remote sensing involves equipment which interacts with the landscape by emitting energy towards the surface and measuring how much is reflected back to the sensor. Microwave imaging can be used to detect land cover and vegetation structure, and also soil water content, through the amount of backscatter detected (Kasischke et al., 2009). Light Detection and Ranging (LiDAR) uses a laser to measure structural changes at the earth's surface, and can therefore be useful in assessing the structure of vegetation. Synthetic Aperture Radar (SAR) can detect ground motion through very precise measurements of Earth surface height, allowing short term elevation changes due to subsidence or oxidisation, seasonal elevation changes due to the gas content of the peat (peat breathing), and other changes in surface texture and vegetation height to be observed (Cigna and Sowter, 2017).

This review focuses mainly on the visible and NIR data, as these are the most useful for estimating carbon fluxes due to their association with plant photosynthesis.

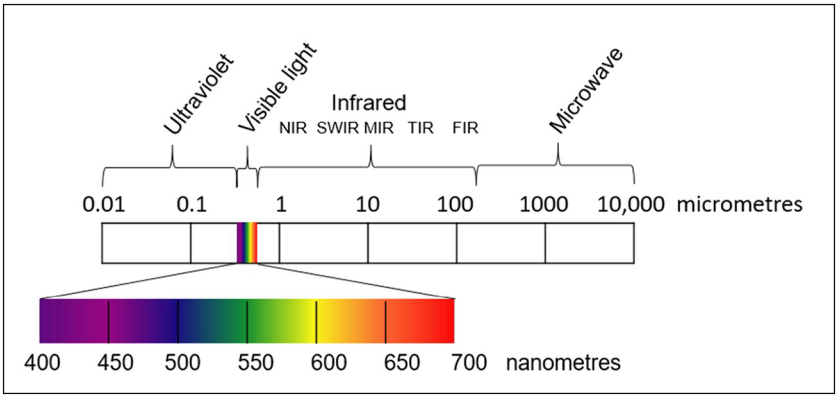

Fig. 4. Diagram of the relevant section of the electromagnetic spectrum.

Table 1
Comparison of satellite sensors used for carbon flux estimation which are mentioned in this review. For key to acronyms please see text and the table of acronyms given at the start of this manuscript.

Satellite (instrument)	Spectral resolution	Spatial resolution	Temporal resolution	Operated by	In operation since	Other notes
Terra and Aqua (MODIS)	0.4 to 14.4 μm (36 bands)	250 m, 500 m, 1 km	1–2 days	NASA	Terra: Dec., 1999, Aqua: May 2002	
Landsat 7 (ETM+)	0.45 to 12.50 μm (8 bands)	30 m	16 days	USGS/NASA	Apr., 1999	Band 8 panchromatic and at 15 m spatial resolution
Landsat 8 OLI and TIRS	0.43 to 12.51 μm (11 bands)	30 m	16 days	NASA/USGS	Feb., 2013	Band 8 at15 m resolution
Sentinel-2 (MSI)	0.44 to 2.19 μm (13 bands)	10 m, 20 m, 60 m	5 days	ESA	Mar., 2017	Vis and IR bands at 10 m spatial resolution; IR and NIR at 20 m.
Sentinel-3A OCLI	400 to 1020 nm (21 bands)	300 m to 1 km	1–4 days	EUMETSAT	Feb., 2016	
Sentinel-3A SLSTR	550 to 12,000 nm (9 bands)	300 m to 1 km	2 days	EUMETSAT	Feb., 2016	
Hyperion	0.4 to 2.5 μm (220 bands)	30 m	16 days	NASA	Nov., 2000 to Jan., 2017	Only source of spaceborne hyperspectral imaging till 2005
WorldView-1	400 to 900 nm (1 band)	0.5 m	2 days	DigitalGlobe	Sep., 2007	Commercial
WorldView-2	0.4 to 1.4 μm (8 bands)	0.3 to 2 m	1 day	DigitalGlobe	Oct., 2009	Commercial
WorldView-3	400 to 2245 nm (28 bands)	0.3 to 3.7 m	1 day	DigitalGlobe	Aug., 2014	Commercial
GOSAT (TANSO-FTS)	0.758 to 14.3 μm (4 bands)	10.5 km diameter footprint	3 days	JAXA	Jan., 2009	Only 2–5% of data usable, detects CH_4, CO_2 in air column
GOSAT (TANSO-CAI)	0.380 to 1.62 μm (4 bands)	0.5 to 1.5 km	3 days	JAXA	Jan., 2009	Only 2–5% of data usable, due to cloud cover.
OCO-2	3 high resolution channels (0.76 μm, 1.61 μm, 2.06 μm)	1.29 km × 2.25 km	16 days	NASA	Jul., 2014	Data impacted by cloud cover; detects CO_2 in air column
SUOMI-NPP (VIIRS)	0.41 to 12.5 μm (22 bands)	357 m, 750 m	2 to 4 days	NASA/NOAA/DoD	Oct., 2011	To succeed MODIS
SPOT 6 & 7	450 to 890 nm (5 bands)	1.5 to 6 m	When commissioned	Spot Image	SPOT 6: Sept 2012, SPOT 7: June 2014	Commercial
MERIS	0.39 to 1.04 μm (15 bands)	260 × 300 m (land)	3 days	ESA	March 2002 to May 2012	No longer in use
FLEX	500 to 780 nm	300 m	1 month	ESA	Not yet launched	
EnMAP	Hyperspectral	30 m	Unknown	German Research Centre for Geosciences (GFZ)	Not yet launched	
HyspIRI	Infrared region	Unknown	Unknown	NASA	Not yet launched	Study phase

There are many satellites now in orbit which are specifically designed for Earth Observation (EO) uses. A selection showing the range of satellite data available to researchers for carbon flux estimation are detailed below and in Table 1.

- Terra and Aqua are satellites run by NASA. Both carry an instrument known as **MODIS** (Moderate Resolution Imaging Spectroradiometer). They cover the majority of the Earth's surface every 1–2 days, and can acquire data in 36 spectral bands (from 0.4 to 14.4 μm) with a spatial resolution of 250 m to 1 km (NASA, 2016a). MODIS is particularly useful in that is has a processing system which creates several data products, including vegetation indices and an estimate of GPP (see Section 2.2.3) using models designed to convert measurements of energy into secondary derived parameters. For most other satellites this processing must be done by the user.
- The **Landsat** program is a series of satellites (Landsat 7 and 8 are currently operating) run by the US Geological Survey (USGS). Each satellite covers the Earth every 16 days, collecting data in several bands within the visible/NIR and TIR wavelengths at a spatial resolution of 30 m for the visible/NIR and 100 m for the thermal bands (USGS, 2016). The first Landsat was launched in 1972. The availability of over forty years of data means that Landsat is especially useful for researchers studying change over time. However, the completeness of the data archive is limited, especially during the 1970s and 1980s.
- **Sentinel-2** is a mission run by the European Space Agency (ESA), consisting of two satellites: Sentinel-2A and Sentinel-2B. Each satellite carries a multispectral imager with image resolution on certain sensors down to 10 m, and when both satellites are operational the return interval is every five days (ESA, 2016). This mission is a continuation of the SPOT and Landsat missions, and similar orbits should allow data from Sentinel-2 to be used as an addition to existing datasets (ESA, 2016). The finer resolution and frequent return interval of this mission should make the data it produces invaluable for a number of land-monitoring applications, including peatland carbon fluxes. Sentinel-1 (SAR) does not currently have a known application in modelling GHG exchange, although it is being used by some researchers to estimate peatland condition.
- **Sentinel-3** also consists of two satellites; Sentinel-3A is already in orbit, and Sentinel-3B is scheduled to be launched in 2018. Sentinel-3 will collect spectral data over land (**Ocean and Land Colour Instrument** (**OLCI**)), and temperature data (**Sea and Land Surface Temperature Radiometer** (**SLSTR**)) every two days (ESA, 2016). Although it has a faster revisit time than Sentinel-2, the spatial resolution is much coarser, being 300 m at best.
- **Hyperion** was an imaging spectrometer on board EO-1 designed to be compatible with Landsat data (and flew in formation with Landsat 7), but had a much higher spectral resolution and could detect 220 bands (0.4 to 2.5 μm) at 30 m spatial resolution (USGS, 2011). This means the data are useful for calculating indices such as the Photochemical Reflectance Index (PRI) and red-edge (see Section 2.2.2), which require a high spectral resolution (Gitelson et al., 2012; Harris et al., 2014; Yu et al., 2014). Hyperion's fine resolution also made it especially useful in heterogeneous environments (Christian et al., 2015). Unfortunately EO-1 has now been decommissioned and only ever captured data on request, but all data which were collected are now freely available.
- **Worldview** is a series of 3 satellites owned by DigitalGlobe, which provide commercial earth observation data. The spatial resolution can be as high as 30 cm, with daily coverage and both multi- and super-spectral bands available (DigitalGlobe, 2016).
- **GOSAT** is a Japanese satellite which carries out column gas abundance measurements using the **Thermal And Near-infrared Sensor for**

carbon Observation (**TANSO**) instrument (composed of the Fourier transform spectrometer (FTS) and the cloud and aerosol imager (CAI) (NIES, 2016). Column gas abundances are calculated by analysing the IR light reflected from the surface compared to the IR light emitted from the atmosphere, allowing the amounts of CO_2, CH_4, H_2O and O_2 to be estimated (NIES, 2016). Column gas abundance satellite missions can be used to estimate CO_2 fluxes by inverting atmospheric transport models. Unfortunately the outputs tend to be very coarse resolution (0.5 to 1.5 km), which makes them less useful for studies of specific land cover types.

- **Orbiting Carbon Observatory 2** (**OCO-2**) is also a column gas abundance mission run by NASA. It has a longer return interval than GOSAT (16 days), and a footprint of 1.29 × 2.25 km. It carries three high resolution spectrometers, with two focused on CO_2 channels, and one on O_2 (NASA, 2016b).

Planned future sensors include: **FLEX** (**Fluorescence Explorer**) which is specifically designed to detect energy at the vegetation fluorescence peaks (see Section 2.2.2.1 for the uses of fluorescence data) (Kraft et al., 2012; ESA, 2015); **EnMAP**, which will carry a hyperspectral sensor and is due to launch in 2018 (EnMAP, 2016); and **HyspIRI** which will focus on the infrared region (NASA, 2016c).

One sensor which is no longer running, but which is mentioned in the following sections of this paper, and for which the data are still available, is the **Medium Resolution Imaging Sensor** (**MERIS**) (ESA, 2017).

2.2. Estimating GPP

There are several techniques using RS data which have been developed to estimate carbon fluxes, and many of the most well-known are explained in this section. It is also important to mention the ground validation techniques which are commonly used to assess the accuracy of these models. The two ways of measuring carbon fluxes directly are flux chambers and EC towers (see Fig. 3). Flux chambers are not often used as a validation method for models using satellite data due to their small coverage. EC towers are more commonly used, and rely on the principle that gas movement in the atmosphere is through turbulent motion. See Section 1 for discussion of the coverage of these two methods, and Section 4 for discussion of some of the problems arising from their use as ground-validation methods.

2.2.1. The LUE model

The most widely used model for estimating GPP from remotely sensed data is currently the **Light Use Efficiency** (**LUE**) model developed by Monteith (1977) (Hilker et al., 2008). The equation for this model is:

$$GPP = fPAR * PAR * \varepsilon$$

where PAR is the total photosynthetically active radiation incident on the vegetation, *f*PAR is the fraction of photosynthetically active radiation absorbed by vegetation, and ε is the conversion efficiency of absorbed energy which is then fixed as carbon within an ecosystem. The product of *f*PAR and PAR is sometimes given as APAR (Absorbed Photosynthetically Active Radiation). PAR is measured as the amount of light within the wavelengths that plants are able to absorb and use for photosynthesis (400 to 700 nm), and can be calculated using weather and climate data (Pfeifer et al., 2012). PAR is affected by cloud cover (Min, 2005), and when considering ground plant species such as mosses, also by the presence of a higher vegetation canopy (Chong et al., 2012). In many LUE models *f*PAR is modelled as a function of a vegetation index, and is often assumed to have a linear relationship with the NDVI (Normalised Differentiation Vegetation Index) (Huemmrich et al., 2010). *f*PAR is also related to Leaf Area Index (LAI) as this partially determines how much energy is absorbed by the canopy (Yuan et al., 2007; Pfeifer et al., 2012). An issue with the relationship between *f*PAR and LAI for *Sphagnum* is in defining an appropriate light extinction coefficient, which is often set to unrealistic values (Weston et al., 2014). ε is often calculated from a constant of εmax for a specific biome (e.g. grassland, forest, cropland) adjusted for limiting factors such as temperature and moisture availability (Garbulsky et al., 2011; Tan et al., 2012). It is also possible to calculate ε directly from the Photochemical Reflectance Index (PRI – see Section 2.2.2).

LUE-based models are very useful because they require few species-dependent parameters, and can be fairly easily calculated from remotely sensed data (Anderson et al., 2008). However, the calculation of ε in many models is considered to be overly simplistic. LUE varies with plant species, ecosystem types, and seasons, and so is unlikely to be accurately represented by a modified constant (Peñuelas et al., 1995).

2.2.2. Vegetation indices

Many EO implementations of the LUE model use a vegetation index (VI) to estimate fPAR, and in some cases to infer other ecosystem properties. VIs can be useful proxies for environmental variables such as water content of vegetation (see Section 3.3), for identifying land cover categories, and in some cases (such as PRI) as a proxy for ε in the LUE model. Below we review some key VIs useful in GPP estimation studies.

One of the oldest and most widely used VIs is the **NDVI** (**Normalised Difference Vegetation Index**), which is calculated from the difference in reflection between the red band and the near-infrared (NIR) band (see Fig. 5). The equation is:

$$NDVI = (NIR - red)/(NIR + red)$$

As healthy green plants absorb light in the red band and reflect it in the NIR band, where there is an abundance of green vegetation the NDVI values will be high. However, the NDVI tends to saturate at high LAI values and is sensitive to the scattering effect of atmospheric aerosols (Walker et al., 2014). The saturation effect can cause a summer plateau in NDVI values in some ecosystems but may not be particularly noticeable in northern peatlands due to the low LAI values of these environments (see Section 3.2).

The **Enhanced Vegetation Index** (**EVI**) is designed to overcome some of the limitations of NDVI. In particular, it includes reflectance in the blue light band to counteract the effect of aerosols, as the light which interacts with these is mostly in the blue portion of the spectrum (Balzarolo et al., 2016), and has generally lower values to compensate for the saturation effect of the NDVI (Heute et al., 2002; Rahman et al., 2005). In general it is agreed that the EVI is a more structural measure, linked to LAI and vegetation canopy structure, as it is more sensitive to NIR (Rossini et al., 2012), whilst the NDVI correlates better with plant chlorophyll content by being more sensitive to the red bands (Heute et al., 2002; Walker et al., 2014). Verma et al. (2015) found that EVI alone, validated against the Fluxnet dataset which included several different ecosystems, gave as much information about seasonal GPP change as the more complex PAR-based models, and as the MOD17 model (see Section 2.2.3). The MODIS product MOD13 contains both NDVI and EVI products.

The **Red Edge Position** (**REP**) index monitors the position of the point of steepest slope between the red and NIR wavelengths in a spectral image (see Fig. 5) (Baranoski and Rokne, 2005). As chlorophyll increases, more red light can be absorbed by the plant and so the red edge moves to increasingly longer wavelengths (Dash and Curran, 2004). Stresses such as low water availability reduce the chlorophyll content and so the red edge shifts to lower wavelengths (Harris et al., 2005). REP is best calculated with narrow-band sensors (e.g. Hyperion – see Section 2.1) which can more accurately determine the position

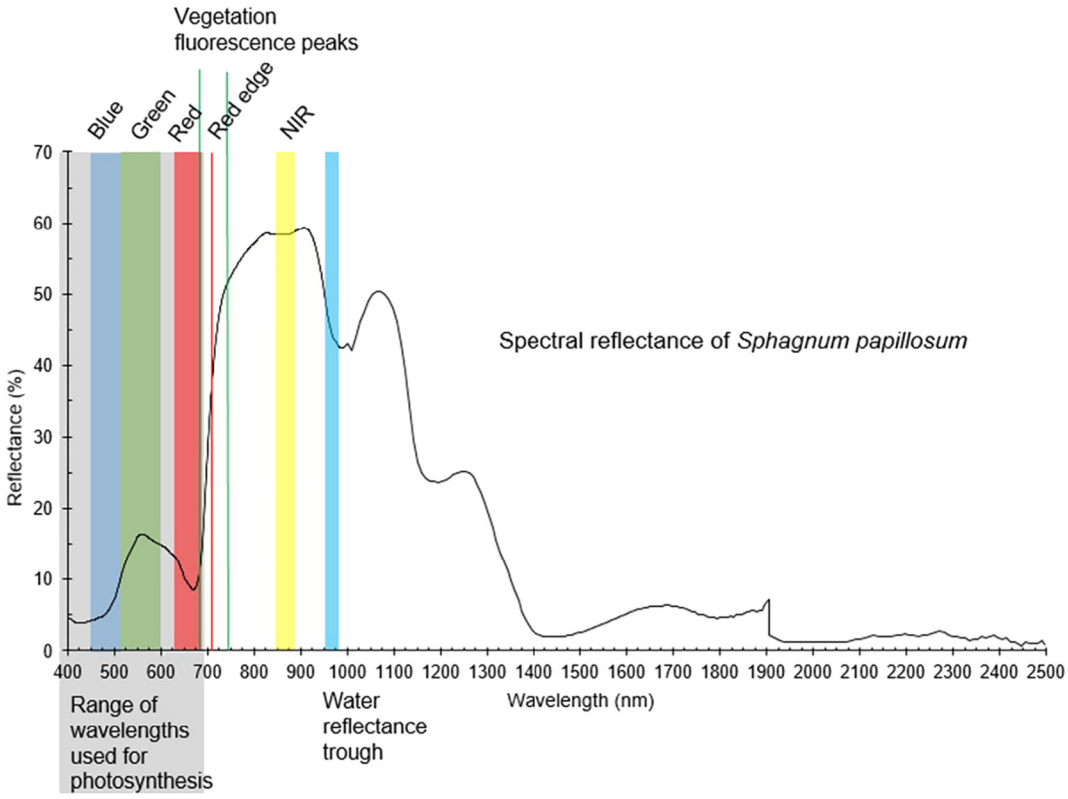

Fig. 5. An example of a spectral reflectance graph of *Sphagnum* moss. The visible and NIR bands follow the wavelengths used by Landsat (blue 450–515 nm; green 525–600 nm; red 630–680 nm; NIR 845–885 nm). Vegetation fluorescence peaks (690 and 740 nm) and the water reflectance trough (950–970 nm, used by the WI) are added. The sample was taken from the Forsinard Flows RSPB reserve and the reflectance was taken in the laboratory using a Ger3700 spectrometer (unpublished data). It is worth noting that the reflectance of *Sphagnum* is greatly impacted by water content, bleaching and increasing reflectance in all wavelengths as it dries.

of the red-edge (Yu et al., 2014), although Dash and Curran (2004) created a successful index known as the MTCI (MERIS Terrestrial Chlorophyll Index), which used this principle on MERIS data (Rossini et al., 2012).

The **Photochemical Reflectance Index** (**PRI**) is a more recent VI development, and measures LUE through a different mechanism than plant greenness. The NDVI and EVI are considered useful proxies for the *f*PAR because they indicate leaf area and chlorophyll amount. The PRI is considered to be a proxy for ε because it measures light-use efficiency directly (Peñuelas et al., 2011; Garbulsky et al., 2011). PRI, and also fluorescence (see Section 2.2.2.1), are based on our understanding of the photoprotective mechanisms within plants. In some circumstances plants will absorb more light energy than can be used by chlorophyll to make glucose. When this is the case, light energy is either transferred to xanthophyll molecules inside the photosynthetic organelles and emitted as heat energy, or emitted as fluorescence (Gamon et al., 1992; Peñuelas et al., 1995). The shift in reflectance associated with increased xanthophyll concentration can be detected at a wavelength of 531 nm by comparison with a reference wavelength. The reference wavelength is often given as 570 nm, although there is some debate (Grace et al., 2007; Van Gaalen et al., 2007; Gamon et al., 1992) about what specific wavelength works best at leaf or canopy scale.

PRI is better than alternative ways of estimating LUE from look-up tables based on vegetation type, as done in many satellite-based LUE models of GPP, because a single measurement already includes environmental constraints and can vary freely across different biomes without the use of categorisation (Peñuelas et al., 2011; Tan et al., 2012). However, PRI requires narrowband sensors with a spectral resolution of 3 to10 nm. One of the biggest issues with the PRI is that the ratio has not yet been standardised across studies, with different wavelengths being used at different sites and scales, which makes cross-comparison difficult (Garbulsky et al., 2011). PRI was originally developed at the leaf level (Gamon et al., 1992) and it is uncertain how well the same wavelengths can be transferred to canopy measurements where scattering affects the signature (Gamon et al., 1992; Peñuelas et al., 1995; Garbulsky et al., 2011).

The high spectral resolution required to accurately calculate PRI means that broad band sensors such as those used on most satellites are not well suited to calculating this index. Hyperspectral sensors cover the spectrum close to continuously, and so have a band centred at 531 nm, whereas most broad-band sensors do not have such a band. MODIS is an exception, however, because Band 11 happens to be centred at around 531 nm (actually 526–536 nm) (Drolet et al., 2005; Goerner et al., 2011). This band has only recently been made routinely available from the Terra satellite (previously it was only processed over the ocean), but it is expected that it will be used in many carbon flux studies over the next few years. There is no band at 570 nm, which means that alternative bands must be used as the reference wavelength. Bands 1 (620–670 nm), 4 (545–565 nm), 12 (546–556 nm) and 13 (662–672 nm) have been found to give reasonable results as reference bands (Drolet et al., 2005; Goerner et al., 2011).

Finally, there are two key points to keep in mind when considering VIs as a proxy for GPP. First, most VIs measure plant greenness rather than actual photosynthesis. Greenness often reaches its maximum before maximum photosynthesis and stressed leaves often reduce photosynthesis without changing colour (Gamon et al., 1992; Grace et al., 2007). Balzarolo et al. (2016) found that the MODIS VIs predict an earlier growing season start date than in-situ EC data suggests, over a range of different ecosystem types, as a result of this effect. Kross et al. (2013) found that this phenological disparity between carbon dynamics and biomass dynamics was evident in four peatland sites of different types, although they suggested that this may be overcome by using an index such as PRI which is more closely related to photosynthetic activity. Second, as well as the problems with the calculation of specific

vegetation indices, all VIs are affected by disturbance from other factors such as topography, observance angle, soil background effects, moisture and atmospheric conditions (see Section 4 for more discussion of these issues) (Peñuelas et al., 2011; Garbulsky et al., 2011; Pfeifer et al., 2012; Walker et al., 2014).

2.2.2.1. Fluorescence. Solar Induced Fluorescence (SIF) is a photoprotective mechanism by which excess light not used during photosynthesis is emitted at longer wavelengths. Although fluorescence can provide useful information about plant stress, the relationship between photosynthetic carbon flux and fluorescence is not simple due to the interaction with the xanthophyll cycle (Harris, 2008). Once plant stress occurs, fluorescence decreases with photosynthesis as the xanthophyll mechanism (measured by PRI) is activated (Meroni et al., 2009). Fluorescence is, however, a good way of detecting photosynthesis changes over short timescales, and responds before chlorophyll abundance or LAI show any change (Meroni et al., 2009).

The two fluorescence peaks in vegetation are at approximately 690 nm in the red bands and 740 nm (see Fig. 5) in the NIR (Meroni et al., 2009; Van Wittenberghe et al., 2015). However, measuring fluorescence requires sensors even finer than those used for PRI, with a resolution of <1 nm (Grace et al., 2007). The precise centre wavelength of the band used also varies slightly with resolution; Meroni et al. (2009) found that a spectral resolution of 0.005 nm was optimal, and anything larger caused a degradation of the signal. As with PRI, fluorescence has been suggested to be more easily measured at leaf level to avoid the canopy scattering and re-absorbance effects (Peñuelas et al., 1995; Van Wittenberghe et al., 2015). Because of the technical challenges associated with measuring fluorescence, almost all previous studies have used ground-based or airborne sensors (Meroni et al., 2009). However, Guanter et al. (2007) showed that space-based fluorescence detection was possible using MERIS. It has also been demonstrated from OCO-2 and GOSAT, as the high spectral resolution used in these sensors is able to pick out the fluorescence signal (Frankenberg et al., 2014). The launch of the ESA FLEX mission will make fluorescence detection over large areas from space much more accessible.

2.2.3. LUE model development

Several models have been developed to estimate GPP, working from the basis of the LUE model and often incorporating vegetation indices as proxies for *f*PAR and/or ε. This section details some of the most well-known models which have been developed over the last two decades, and compares their model formulations and variables in Table 2.

Early GPP models such as CASA (Potter et al., 1993) and 3-PG (Landsberg and Waring, 1997) combined satellite data with field data such as meteorological inputs and soil/vegetation types. The first model to rely solely on remotely sensed data was the **Global Production Efficiency model** (**GLO-PEM**) (Prince and Goward, 1995). GLO-PEM uses data from the AVHRR (Advanced Very High Resolution Radiometer) to calculate a basic LUE model with a developed ε parameter. ε_{max} is given a different value for C3 and C4 plants, and modified by air temperature, Vapour Pressure Deficit (VPD) and soil moisture (Prince and Goward, 1995). VPD is calculated as the difference between the saturation point of air and the current water vapour in the air, and is linked to carbon fluxes through the relationship between photosynthesis and evapotranspiration (Shurpali et al., 1995). GLO-PEM was an important step forward, but as the first fully RS-reliant model it should be considered as method development, and many further improvements have been made in later models. In particular, Tan et al. (2012) found that GLO-PEM's generalisations of plant categories only poorly account for ecosystem variation.

The **terrestrial Vegetation Photosynthesis Model** (**VPM**) is a modified LUE model which uses the Land Surface Water Index (LSWI) as a modifier of ε. The *f*PAR is calculated as a linear function of the Enhanced Vegetation Index (EVI), and attempts to solve problems created by non-photosynthetic vegetation registering as photosynthetically active in remote sensing data (Xiao et al., 2004). Dong et al. (2015) found that the VPM was the best model for explaining variance in cropland and prairie under drought conditions, and attributed this to the combination of EVI and a water content index. Dong et al. (2015) also pointed out, however, that the VPM requires more data inputs than simpler models and so cannot be used in places where there is no meteorological data. The VPM has been validated over a number of different ecosystems and has been shown to give good results using data from several satellite sensors, including both MODIS and Hyperion (Xiao et al., 2004; Christian et al., 2015). The VPM was used over peatlands by Kross et al. (2016), as is discussed in more detail in Section 3.2.

The **EC-LUE** (**Eddy Covariance LUE model**) is so named because it is a modified LUE model which was developed using the latent heat flux measured by EC towers in its calculation (Yuan et al., 2007). The model relies on air temperature and evaporative fraction (EF) to modify LUE. Interestingly, the model constrains GPP by either temperature or water deficiency, depending on which is most limiting (Yuan et al., 2007). In the original 2007 model the EF was calculated using latent heat flux and the Bowen ratio (Yuan et al., 2007), but later versions of the model use net radiation from climate observation networks, modified by evapotranspiration parameters (Yuan et al., 2010). This means

Table 2
Simplified description of well-known RS GPP models, and their major strengths and weaknesses for use over peatlands.

Model	Equation	Source of fPAR	Source of other variables	Strengths and weaknesses	Reference
MOD17	$GPP = fPAR \times PAR \times (E_{max} \times f(T_{min}) \times f(VPD))$	From LAI (MOD15)	VPD (Vapour Pressure Defecit - determined from land cover MOD12) Tmin (minimum temperature from GMAO)	Strength: No site optimisation needed Weakness: No peatland classification	Running and Zhao, 2015
GLO-PEM	$GPP = fPAR \times PAR \times (E_{max} \times Ta \times VPD \times$ soil moisture)	NDVI	Ta (air temperature from NDVI and LST relationship) Soil moisture (from NDVI and LST relationship) VPD (vapour pressure deficit from thermal infra-red)	Strength: First fully RS-based model Weakness: Broad plant category generalisations	Prince and Goward, 1995
VPM	$GPP = fPAR \times PAR \times (Emax \times Ts \times Ws \times Ps)$	EVI	Ts (air temperature scalar from ground data) Ws (water scalar from LSWI) Ps (leaf phenology scalar based on deciduous/evergreen and LSWI relationship)	Strength: Validated under drought conditions Weakness: Requires meteorological data	Xiao et al., 2004
EC-LUE	$GPP = fPAR \times PAR \times (Emax \times \min(Ts, Ws))$	NDVI	Ts (air temperature scalar from ground data) Ws (water scalar, from evaporative fraction)	Strength: Validated across a wide range of ecosystems Weakness: May overestimate GPP at moss-dominated sites	Yuan et al., 2007, 2010
TG	$GPP = EVIs \times LSTs \times m$	–	LSTs (land surface temperature scalar) EVIs (enhanced vegetation index scalar) m (unit scalar)	Strength: Only requires two inputs Weakness: No water stress component	Sims et al., 2008

that the model can now be applied to large areas without tower data, and has also been shown to be more accurate than the 2007 EC-LUE model (Yuan et al., 2010). The EC-LUE model was validated against fifty-four sites with EC towers, but these sites only covered six major biomes, and did not specifically include peatland or wetland sites. Yuan et al. (2010) found that the model overestimated GPP at high latitude sites, and suggested that this may be caused by a high proportion of mosses which have a lower LUE than vascular plants.

Temperature and greenness (TG) models are a general class of satellite based GPP models which use land surface temperature (LST) as a proxy for other environmental variables in the LUE equation. A recent example is that of Sims et al. (2008) which only includes LST and EVI, and is therefore easily calculated from MODIS products. Sims et al. (2008) found that the LST dataset from MODIS correlates well with both PAR and VPD, and can therefore be used as a remotely sensed proxy. Their results showed that the TG model performed better than MOD17 across a range of North American biomes, but noted that it performs significantly less well at sites where vegetation is sparse (Sims et al., 2008). Verma et al. (2015) found that the TG model performed as well as more complex models when compared to EC data from the Fluxnet dataset across several different biomes. However, Dong et al. (2015) point out that it does not include any water stress modifier and so estimates variance in drought years rather poorly.

NASA uses MODIS data to produce an estimate of GPP. This product, which has been assigned a data code of **MOD17**, uses a modified version of the LUE algorithm to produce an 8-day total GPP at 1 km resolution across the globe (Running and Zhao, 2015). The difference between the MOD17 product and other LUE models is that it uses modelled processes rather than vegetation indices to calculate *f*PAR. This MOD17 *f*PAR is taken from the MODIS LAI product (MOD15), which is generated by inversion of a physical model of light scattering in the plant canopy against observed MODIS reflectance data. Daily meteorological data from the NASA Global Modelling and Assimilation Office (GMAO), including Vapour Pressure Deficit (VPD) and minimum temperature, are used to calculate PAR, and also to limit ε_{max} (Running et al., 2004; Tan et al., 2012; Running and Zhao, 2015).

Several studies have attempted to analyse the accuracy of the MOD17 product for different biomes and have concluded that there are inherent errors associated with the meteorology, radiometry and biophysical inputs. Heinsch et al. (2006) found that the largest source of error across fifteen sites in different biomes across North America was the VPD, which is calculated from NASA/GMAO data and used as a drought proxy to limit ε. In MOD17 VPD was found to often be underestimated, leading to a GPP overestimation compared to EC tower data (Heinsch et al., 2006). Another source of error in ecosystem studies is that the MOD17 εmax and the limits of VPD and temperature are estimated from the MODIS land cover classification product, MOD12Q (Tan et al., 2012). MOD12Q has a limited number of land cover classifications (see Table 3). This can cause errors in GPP estimation. It can be seen (Table 3) that there is no specific class for peatlands. This means that peatlands as a whole are classified as other land cover types. Such land-cover types almost certainly do not possess the high percentage of organic matter and waterlogged conditions so characteristic of peatland ecosystems. Kross et al. (2013) found that northern peatlands were often misclassified as evergreen needleleaf forest, mixed forest, or closed shrubland. Finally, Tan et al. (2012) point out that the MOD17 product does not include any estimate of surface moisture, which may particularly limit its usefulness when used on peatland sites. Some peatland species rely on high surface moisture for their water inputs, and including this factor in models can help to assess desiccation effects on photosynthesis (see Section 3.3).

Table 3
MOD17 land cover types, from Running and Zhao (2015) p11. Note there is no peatland/wetland category.

Class value	Class description
0	Water
1	Evergreen needleleaf forest
2	Evergreen broadleaf forest
3	Deciduous needleleaf forest
4	Deciduous broadleaf forest
5	Mixed forest
6	Closed shrubland
7	Open shrubland
8	Woody savanna
9	Savanna
10	Grassland
12	Cropland
13	Urban or built-up
16	Barren or sparsely vegetated
254	Unclassified
255	Missing data

2.3. Estimating ecosystem respiration

To obtain a full picture of ecosystem carbon exchange (i.e. to estimate NEE), we need both an estimate of GPP and an estimate of ecosystem respiration (R_{eco}). Ecosystem respiration is a combination of two sources of respiration: autotrophic respiration (Ra) from the plants themselves, and heterotrophic respiration (Rh) from microbiota within the soil (Fig. 1). Ra consists of maintenance respiration and growth respiration, whilst Rh consists of rhizomicrobial respiration, and microbial decomposition of plant residues and other soil organic matter (SOM) (Gao et al., 2015). There are far fewer successful models of ecosystem respiration (R_{eco}) compared to GPP because it is much harder to account for the variation found between ecosystems, particularly using RS (Olofsson et al., 2008; Jägermeyr et al., 2014).

Many models produce an estimate of NPP, which is the difference between GPP and Ra. In LUE-based models maintenance and growth respiration can be accounted for as part of the ε parameter (Running et al., 2004) but there are fewer models which seek to estimate respiration directly, and particularly soil (heterotrophic) respiration. Despite this, several studies have suggested that the relationships between R_{eco} and GPP (Vourlitis et al., 2003) and R_{eco} and temperature (Rahman et al., 2005; Olofsson et al., 2008) are strong enough to estimate R_{eco} from RS data. Some models use a Q_{10} function, which gives a change in sensitivity of respiration to temperature with every 10° (Reichstein et al., 2003). Some studies and models which include soil respiration are discussed below, and listed in Table 4.

Reichstein et al. (2003) found that soil water and temperature were good predictors for soil respiration. They also found that adding LAI as a proxy for productivity to the model improved the result. Their study was based on closed-chamber data from forest and shrubland sites across Europe and North America, but it was suggested that the variables could easily be estimated from RS data. This was proved to be the case by Anderson et al. (2008) who used a model which calculated soil moisture from microwave sensing, soil temperature from thermal imaging, and LAI from a vegetation index. Their model results showed good agreement with tower flux data over pasture land in Oklahoma (Anderson et al., 2008). Model development over such a small area, however, is unlikely to create a model which is reliable over other ecosystems or climates, and more validation work is needed.

Turner et al. (2006) created a model which estimates both Ra and Rh. The Ra portion of the model calculates maintenance respiration using a base rate and a Q_{10} function, while the growth respiration equation is based on the fraction of carbon available for growth (given as 0.33) used in respiration. Rh is calculated using a base rate modified by in-situ measurements of soil temperature, soil moisture and stand age. Both maintenance respiration and heterotrophic respiration are scaled by *f*PAR as a proxy for live biomass (Turner et al., 2006). Turner et al. (2006)'s model shows potential for a fully remote sensing based model, but also relies on data from a process-based model and in-situ data.

Table 4
Respiration models and their major strengths and weaknesses for use over peatlands.

Model	Equation	Variables	Strengths and weaknesses	Reference
Anderson et al., 2008	$Rh = (0.135 + 0.054 \times LAI)\theta_{10}\exp[0.069(T_{s,10}–25.0)]$	LAI (from vegetation index) θ_{10} (the 0 to 10 cm average volumetric water content, derived from microwave data) $T_{S,10}$ (the 10-cm soil temperature, derived from thermal band imagery)	Strength: Fully RS based Weakness: Only developed over pasture land	Anderson et al., 2008
Turner et al., 2006	$Rm = Rm\_b \times Q_{10}{}^{((Tair\ -\ 20)\ /\ 10)} \times (1/-k)(\log(1-FPAR)$	R m_b (base rate of maintenance respiration, from model) Q_{10} (change in rate for a 10 °C increase in temperature, 2.0 used by Turner et al., 2006) Tair (daily (24 h) mean air temperature from database) k (radiation extinction coefficient, 0.5 used)	Strength: Calculates Rh and Ra separately Weakness: Relies on in-situ data	Turner et al., 2006
	$Rg = (GPP - Rm) \times Rg\_frac$	Rg_frac (fraction of carbon available for growth that is used for growth respiration (0.33, Waring and Running, 1998))		
	$Rh = Rh\_base \times S_{ST} \times S_{SW} \times S_{SA} \times FPAR$	Rh_base (base rate of heterotrophic respiration, from model) S_{ST} (scalar for soil temperature from database) S_{SW} (scalar for soil water content from database) S_{SA} (stand age factor from Landsat data)		
Wu et al., 2014	$Rh = a(NDVI \times LST_n) + b$	LST_n (night time LST) a = slope (related to annual LAI max) b = intercept (related to annual LAI average)	Strength: Simple to use Weakness: No soil water parameter	Wu et al., 2014
RECO	$Re_{ref} = p1 + p2 \times EVI_{mean} + p3 \times LST_{mean}$ $Re_{std} = (p4 / (p5 + p6 - ((LST_n - 10) / 10)) + p7 \times EVI + p8$	EVI_{mean} (mean annual springtime EVI) LST_{mean} (mean annual daytime LST) LST_n (night-time LST) EVI (8-day EVI/EVI_{mean})	Strength: Good results across the Fluxnet network Weakness: Limited biome classification	Jägermeyr et al., 2014
ReRSM	$Re = a \times GPP + R_{ref} \times e^{E_0 \times ((1\ /\ 61.02)\ -\ (1\ /\ T\ +\ 46.02))}$	R_{ref} (EOM-derived respiration at reference temperature) T (average of daytime and night-time LST)	Strength: Excellent model performance over Tibet and Northern China Weakness: Only validated over limited ecosystems	Gao et al., 2015

Wu et al. (2014) used NDVI and LST from MODIS to calculate soil respiration, along with two further parameters determined from site LAI. They found that night-time LST is more useful as it is a less noisy signal than daytime LST. Their model explained 78% of variance in eight years of flux data from a Canadian forest, but was limited by the lack of a soil water variable.

Jägermeyr et al. (2014) designed the **RECO** model to estimate global respiration. They assigned the world's ecosystems to one of three climate zones, each zone then being divided into further sub-categories of forested and non-forested biomes. Different model parameters were then created for each category. The model equation has two components: R_{ref} which is the reference respiration (calculated from yearly means of EVI and LST), and R_{std} which is the seasonal variation in the ratio of R_{ref} to R_{eco} (calculated using night-time LST, EVI and the difference between day and night LST as a soil water proxy in water-limited biomes). The model results were compared with several different sites across the Fluxnet network to give an R^2 value of 0.62. The limited classification of biomes in the model, however, means that parameterisation may not take into account the wide variety of ecosystems that were not specified. This may be acceptable for a global model, but could cause large errors if applied to a specific ecosystem without additional parameterisation.

Gao et al. (2015) created the model **ReRSM**, which separates R_{eco} into GPP derived components (growth and rhizomicrobial respiration) and ecosystem organic matter (EOM) derived components (maintenance respiration, respiration from decomposition of plant residue and other SOM). The GPP component is calculated using EVI and LSWI (Land Surface Water Index). The EOM contribution to total respiration is calculated using the Lloyd-Taylor model which is another exponential function which relates temperature and respiration (Lloyd and Taylor, 1994) calculated from MODIS LST (Gao et al., 2015). They found that this model could explain 90% of the variation in respiration from EC data over five different ecosystem types in Northern China and the Tibetan plateau, with a root mean squared error (RMSE) of 0.05. These numbers suggest an excellent model performance, but cannot necessarily be transferred well to other ecosystem types, and may particularly be less accurate in areas affected by drought as there is no soil water component affecting the EOM derived respiration (Gao et al., 2015).

These GPP and R_{eco} models were all developed on ecosystems other than peatland, and future application of these models to peatland areas will require an assessment of the effect of parameters such as temperature and soil moisture on respiration in different peatland types (see Hilker et al., 2008 and Tan et al., 2012 for reviews of GPP models over other ecosystems).

3. Previous studies on peatlands

Remote sensing studies of peatland carbon fluxes can be placed into two broad categories: classification studies, which divide the landscape into types with similar conditions, and carbon flux estimation studies using models such as those explored in Section 2 (Whiting, 1994).

3.1. Classification studies

Classification studies can be used both to identify peatland as a distinct land use (in comparison with areas of forest or agricultural land for example) and also to identify vegetation communities and topographic features within a peatland environment. These classification studies can then be used to define key parameters (e.g. ε_{max}) in order to adjust a general model to specific conditions.

Peatlands are often classified in RS studies on the basis of vegetation types. Different plant species dominate under different conditions, and can affect the carbon fluxes of the peatland. A higher proportion of vascular plants to mosses increases both photosynthesis and autotrophic respiration and is also likely to be associated with an increase in heterotrophic respiration because a larger amount of available substrate is present (Limpens et al., 2008; Dinsmore et al., 2009; Walker et al., 2016). It is important to note that different vegetation compositions on peatland differ not only in their overall NEE, but also in the response of their carbon fluxes to environmental change (Bubier et al., 2003). Bubier et al. (2003), for example, showed that sedge-dominated communities within a bog experienced a greater decrease in photosynthesis under drought conditions than communities dominated by ericaceous shrubs in the same ecosystem. It is therefore important to have an understanding of vegetation communities and differential responses when creating a carbon flux model. Some carbon flux estimations can

be achieved simply by applying knowledge of differential responses to land cover and climatic data, as can be seen at a large scale in MOD17.

Several studies have considered the heterogeneity of peatland vegetation at different scales, and have developed ways of classifying areas of differing vegetation composition based on spectral reflectance and structural data – these are not specifically discussed here but can be found in papers such as Bubier et al. (1997), Frolking et al. (1998), Thomas et al. (2003), Anderson et al. (2009), Forbrich et al. (2011), Crichton et al. (2014), and Parry et al. (2015).

3.2. Carbon flux estimation studies

Relating remote sensing directly to peatland carbon fluxes is an area of research which is growing rapidly, although as yet there are still only a few published studies from this increased research activity and therefore any conclusions must necessarily be of a tentative nature. Some studies have used the MOD17 GPP product compared with data from flux towers, but have found that this product has poor accuracy over peatland environments (Schubert et al., 2010; Kross et al., 2013). Kross et al. (2013) found that the MOD17 product underestimated Eddy Covariance GPP at three of their four sites across Canada and Finland (one bog and two fen). They suggest this is due to the unsuitability of the εmax downscaling algorithm in peatland ecosystems. Connolly et al. (2009), however, showed that the MODIS *f*PAR product had a good relationship with *f*PAR derived from field-based LAI measurements. This suggests that although the MOD17 product may provide a good structural analysis and estimate of potential photosynthesis, it is held back by the algorithms for establishing LUE, which are not calibrated well within peatland environments. Kross et al. (2013) suggest that the VPD modifier of LUE in the MOD17 product may be particularly unnecessary over peatlands, as it appears to have had little effect during their study period, and does not have much of a relationship to soil moisture (Harris and Dash, 2011).

Other studies have used vegetation index models as an estimate for field flux data (see Table 5). Harris and Dash (2011) compared MTCI, which uses the red-edge principle, to GPP observations at a raised bog and a moderately rich treed fen and found that there was a good relationship in the active growing seasons of 2004 and 2005 for both sites. Unfortunately, they did not compare this to the performance of other vegetation indices, although the MTCI principle is similar to the NDVI. Kross et al. (2013) considered MODIS NDVI at one raised bog site and three different fen sites, and found that the relationship between NDVI and GPP observations was good at capturing interannual variation at individual sites, and that moreover the same regression coefficient (for NDVI and GPP observations) could be used at several sites with similar characteristics. This suggests that NDVI would be a useful vegetation index in developing a peatland RS model which could be used without site-specific calibration. Harris and Dash (2011) give the R^2 value for a 1:1 relationship between MTCI and GPP values as 0.71 (0.46–0.87), whilst Kross et al. (2013) give the R^2 value for NDVI and GPP as 0.43 (0.39–0.71). These are not directly comparable, however, as the studies were over different sites and time spans, and because the MTCI uses MERIS data whilst Kross et al. (2013) used MODIS NDVI.

Whiting (1994) give a positive correlation value between NDVI (measured in the field using a handheld spectroradiometer) and NEE of 0.43 (using chamber data) over a combination of bog and fen sites, but observed unexpectedly high NDVI values at a site which had a large proportion of brown-green *Sphagnum* species present, and suggest that the differing combinations of moss and vascular plants may complicate the NDVI:NEE relationship. Levy and Gray (2015) studied a peat bog site in Northern Scotland and found only a low correlation coefficient of 0.23 between EC GPP and MODIS NDVI. These studies suggest that NDVI can give us some information about peatland carbon flux, but more factors are needed to create an accurate model on a large scale.

Schubert et al. (2010) compared MODIS NDVI and EVI as predictors of GPP across a raised bog and a minerotrophic fen in Sweden and found that EVI gave better results (R^2 values of 0.37 and 0.45 compared to 0.26 and 0.36). In particular, they noted that the NDVI curve levelled off in summer, indicating saturation. Letendre et al. (2008) completed a study using a handheld spectroradiometer which found that the R^2 value for NDVI and NEE at their *Sphagnum*-dominated open raised bog site in Canada was as low as 0.12, but that combining NDVI with PRI gave a better result (R^2 of 0.26). Letendre et al. (2008) discovered that the Chlorophyll Index (CI, based on red-edge position) gave the best correlation with NEE, with an R^2 of 0.37. Van Gaalen et al. (2007) and Harris' (2008) laboratory studies found that PRI was a good indicator of short term (minutes to hours) changes in photosynthetic efficiency within individual *Sphagnum* species, but required a priori knowledge of the species present. This means it may provide good results under laboratory conditions, but may not translate well to larger scale field studies with the intermixture of *Sphagnum* species present in field conditions. *Sphagnum* patches of a single species rarely exceed 20 cm^2, and it is common to find species entirely intermingled to the extent that even a fine resolution spectrometer would pick up reflectance signals from more than one species.

Kross et al. (2016) considered the variation of the LUE parameter ε over different peatland types in Canada and Finland (same sites as Kross et al., 2013). They found that monthly variations in ε correlated with variations in air temperature and MODIS NDVI, and that annual variations correlated with wetness as measured using LSWI. They also applied the VPM to their study sites, and found good agreement between ε calculated using MODIS data to drive the VPM, and ε calculated using ground-measured data. Unfortunately they did not publish the carbon flux estimates from the VPM.

3.3. Temperature and water content

The two variables most widely considered to affect peatland GPP are soil moisture/Water Table Depth (WTD) and temperature (Harris and Dash, 2011). However, there are issues with including these in RS-driven models as there is debate over whether RS indices can

Table 5
Simple vegetation indices using NIR and red bands (NDVI and MTCI) compared to ground measurements of carbon flux. This table highlights the difficulty of comparing across studies due to different methods of carbon flux and spectral measurement.

Study	Site type	Comparison	R2	CO_2 data	Spectral data
Whiting, 1994	Coastal fen, interior fen and bog	NEE:NDVI	0.18	Chamber	Field spectroradiometer
Letendre et al., 2008	Open raised bog	NEE:NDVI	0.12	Chamber	Field spectroradiometer
Schubert et al., 2010	Raised temperate ombrotrophic bog	GPP:NDVI	0.26	Eddy Covariance	MODIS 250 m
Schubert et al., 2010	Boreal oligotrophic minerotrophic fen	GPP:NDVI	0.36	Eddy Covariance	MODIS 250 m
Harris and Dash, 2011	Raised bog	GPP:MTCI	0.74	Eddy Covariance	MERIS 1 km
Harris and Dash, 2011	Moderately rich treed fen	GPP:MTCI	0.77	Eddy Covariance	MERIS 1 km
Kross et al., 2013	Raised ombrotrophic bog	GPP:NDVI	0.71	Eddy Covariance	MODIS 250 m
Kross et al., 2013	Moderately rich treed fen	GPP:NDVI	0.66	Eddy Covariance	MODIS 250 m
Kross et al., 2013	Open minerotrophic moderately rich fen	GPP:NDVI	0.64	Eddy Covariance	MODIS 250 m
Kross et al., 2013	Mesotrophic sub-arctic poor fen	GPP:NDVI	0.39	Eddy Covariance	MODIS 250 m
Levy and Gray, 2015	Blanket bog	GPP:NDVI	0.09	Eddy Covariance	MODIS 250 m

adequately represent these variables, and therefore to what extent including them improves a model (Connolly et al., 2009; Schubert et al., 2010; Harris and Dash, 2011).

Harris and Dash (2011) found that adding LST to their MTCI-based model did not greatly improve results. They suggest that this may be due to the poor performance of LST as a proxy for more stable soil temperatures, but allow that it may be a useful VPD proxy, and therefore more valuable under drought conditions. In contrast, Schubert et al. (2010) found that adding LST to their EVI-based model did improve results, and also gave a good correlation with R_{eco}. Harris and Dash (2011) based their work on a raised bog and a moderately rich treed fen in Canada, whereas Schubert et al. (2010) were working on a raised ombrotrophic bog and an oligotrophic minerotrophic fen in Sweden – both used EC data as a ground validation method.

Soil water content is likely to be a particularly important model variable in peatland environments as these ecosystems rely on exceptionally high water tables to function. In a natural bog the catotelm will remain saturated all year round, whilst the acrotelm experiences fluctuations (see Fig. 1). Even a small drop in the water table can impact productivity, because *Sphagnum* moss is particularly sensitive to moisture availability. It is also important to note that damaged peatlands and those undergoing restoration may experience much greater fluctuations than natural bog.

Zhang et al. (2015) make the point that the effect of water content on LUE is complex, and different indices may provide additional information within one model. Several studies (Vogelmann and Moss, 1993; Bryant and Baird, 2003; Harris et al., 2005, 2006; Van Gaalen et al., 2007) have shown that the spectral reflectance of several *Sphagnum* species changes as the mosses respond to different moisture conditions – in particular, reflectance increases as the *Sphagnum* dries and becomes paler. *Sphagnum* has very pronounced water absorption features at 990 and 1200 nm (Harris et al., 2005, 2006). The subject of measuring peatland water content from remote sensing data could provide enough material for an entire paper in itself, so a brief summary is all that is given here (see Harris and Bryant, 2009 for more information).

Water indices, as with vegetation indices, can be calculated using visible and infra-red data from satellites. The Water Index (WI) studies the changes in the reflectance trough at 950–970 nm (see Fig. 5), which is caused by the light absorbance of water in plants, compared to a reference wavelength at 900 nm (Peñuelas et al., 1997). The Land Surface Water Index (LSWI), also known as the Normalised Difference Water Index (NDWI) uses the principle that the SWIR band at 1.24 μm measures both water content and other plant factors, whereas the NIR band at 0.86 μm only responds to factors other than water content – the difference is therefore an index of vegetation water content (Gao, 1996). The floating Water Band Index (fWBI) considers the minima between 930 and 980 nm to be the water absorption band. This minimum is compared to the reference wavelength at around 900 nm (Strachan et al., 2002; Harris, 2008).

McMorrow et al. (2004) and Meingast et al. (2014) used specific bands (1400 and 1940 nm; 970, 1200, 1450, 1950 and 2250 nm) to indicate water content and estimate WTD. Meingast et al. (2014) found that the bands in the NIR range gave the best results over vegetated peat. This corroborates Harris et al. (2005)'s work which found that water indices using the NIR range gave the best results in their laboratory work on *Sphagnum* drought stress. Letendre et al. (2008) found that both the LSWI and the WI had strong correlations with volumetric water content in peat (Pearson's coefficients of 0.77 and 0.75 respectively). They also found that using a ratio of NDVI/WI improved the relationship between the vegetation index alone and NEE values at their study site in Canada (Letendre et al., 2008). Harris (2008) found that the fWBI correlated very well with the pooled data for photosynthetic efficiency from five different *Sphagnum* species under drought stress (correlation coefficients of 0.58–0.90). Overall, studies show that water indices using the visible and NIR wavelengths are adequate proxies for water content in the vegetation and acrotelm of bog environments, although passive RS is unlikely to give much information about water contents deeper in the soil. There is no consensus as yet on which is the best, and it may be the case that different indices are better suited to different peatland landscapes and vegetation communities.

4. Challenges of working with RS on peatlands

Remote sensing of peatland vegetation can be a challenge when there are both vascular plants and mosses present at a site, due to the different heights of the species. It can be difficult to accurately measure LAI when there is vertical heterogeneity in the vegetation (Garrigues et al., 2008), and if there is a thick vascular canopy the presence and spectral signal of *Sphagnum* can sometimes be missed altogether (Parry et al., 2015). This height differentiation can also cause a difference in the PAR received by different plants (Chong et al., 2012). Huemmrich et al. (2010) suggest that at some sites it is necessary to treat peatlands as a two-level environment, with a moss understory and a vascular canopy, and to include this distinction in remote sensing models.

The response of *Sphagnum* mosses to environmental conditions is spectrally very different to that of vascular plants. Reflectance in the SWIR regions of the spectrum is lower than for vascular plants due to the higher water content of *Sphagnum* (Bubier et al., 1997; Bryant and Baird, 2003). Calculating NDVI over peatlands has shown unusually high values compared to vascular plant communities, and this can affect GPP estimates in peatlands where *Sphagnum* is prevalent (Whiting, 1994; Letendre et al., 2008). Different plant types also have differing spectral responses to drought (Bryant and Baird, 2003; Lund et al., 2010; Urbanová et al., 2013). Yuan et al. (2014) adjusted the EC-LUE model over boreal forests to take into account the presence of mosses and their effect on GPP estimations. They found that a model with separate εmax values for vascular plants and mosses, and an estimation of proportional contribution to the satellite signal from each, gave a more accurate result (Yuan et al., 2014). Letendre et al. (2008) suggest that the *Sphagnum* challenge may be at least partly overcome by including a water index in any given model.

The prevalence of different vegetation species is strongly related to the type of peatland being studied. There is some evidence that the difference between types of peatland is great enough to affect the relationship with spectral data (see Section 3.2), but as yet there are not enough studies available to quantify this difference. Correctly identifying peatland type and relating this to spectral data is important for generating accurate estimates of carbon flux.

Many peatlands are water-saturated for a large proportion of the year, which can cause problems for remote sensing. High water content may cause an increase in light scattering, or a change in absorption features, which will affect the satellite signal. Also, many of the models discussed (e.g. MOD17, GLO-PEM, EC-LUE, VPM, Turner et al., 2006; Anderson et al., 2008) in this paper assume that a lack of water is a limiting factor on GPP and R_{eco}. However, healthy peatland environments almost always have a very high water table so the water factors in many of these models developed in other ecosystems may need to be re-evaluated for peatlands. Another aspect these models do not consider is that complete saturation is a limiting factor on soil respiration in peatland environments.

Peatland environments are often very cloudy, which can limit the data available from remote sensing. This is an issue with all remote sensing in the visible and infrared wavelengths, but is a particular problem in some ecosystems such as high latitude wetlands. One of the ways to deal with this issue is to use data from a satellite which has a frequent pass interval (e.g. MODIS, Sentinel-3), as there is then a higher chance of collecting a reasonable amount of useful data which can be gap-filled sensibly. The trade-off here is in terms of spatial resolution. Other options include using active sensors which can penetrate cloud cover, or utilising aerial imaging which can be obtained by flying below the cloud layer – though shadows and low light may then become major

factors. One issue associated with cloud cover is that the GPP estimated from RS data may be overestimated if only clear day estimates are used. The range of LUE values is generally much smaller on clear days than on cloudy days – and peatlands occur most widely in areas of high cloud cover (Drolet et al., 2005).

The microtopography of peatlands (see Fig. 2) can also affect carbon fluxes (Bubier et al., 2003; Forbrich et al., 2011), but is difficult to detect directly with RS, particularly when spatial resolution is coarse (Crichton et al., 2014). Waddington and Roulet (1996) found that the scale from which extrapolation is attempted can affect whether the overall estimate is a sink or a source – variation in fluxes is greatest at the microtopography level, although there are also carbon flux variations at the mesoscale due to features such as pools and sections of different land cover. Pools in particular are an important component of the carbon cycle on peatlands, and ignoring their presence may lead to an inaccurate estimate of NEE (Waddington and Roulet, 1996; Lindsay, 2010; Turner et al., 2016).

There are several ways to solve the heterogeneity issue; the first is to use very fine resolution imagery which can detect different vegetation communities, and use this data to analyse the proportion of land which is hummocks and hollows in order to estimate variations in carbon flux within the cells of coarser resolution data (Forbrich et al., 2011). The second is to assume that although peatland is heterogeneous at a small scale, peatland sites are fairly homogenous at a larger scale (this is known as a repeat mosaic). In other words, the assumption is that the grid square size covered by satellites such as MODIS will be a reasonably representative sample of the entire peatland area. A third option is to downscale data from a coarse resolution satellite. There are several methods for downscaling (e.g. Hill et al., 2011; Stoy and Quaife, 2015), one of which is the model STARFM (Spatial and Temporal Adaptive Reflectance Fusion Model) which combines Landsat data (which has fine spatial resolution but a long pass interval, with data from MODIS (which has a coarse spatial scale but short pass interval), to create a product with fine resolution and a short repeat interval (Gao et al., 2006; Walker et al., 2014).

Validation of remote sensing carbon flux models is usually performed using data from EC towers, but there can be issues with scale and geolocation (see Fig. 3). Both EC footprints and satellite pixel sizes can vary. EC footprints change size and shape with wind direction and speed, whilst satellites typically collect data from a slightly different area on each pass, and require geo-correction (Schubert et al., 2010; Harris and Dash, 2011). Clearly, the larger the area covered by the EC footprint, the more chance there is of being able to match it to a satellite pixel (see Fig. 3). The assumption that peatlands are fairly homogenous at large scales and that one satellite point or EC footprint is representative of the whole landscape is necessary for this validation to be meaningful. More work is needed to determine whether or not this assumption can be considered reasonable.

Every method of calculating carbon flux is subject to its own errors, including RS, EC and chamber techniques. For optical sensors in satellites, corrections for atmospheric effects must be made before the data are used. The translation of raw RS data into products and models also introduces error. Data from EC towers, in the form which is often used for validation of RS models, are the result of a series of processing steps which include calculating the flux from the raw turbulence and gas concentration data; averaging the flux over time periods; removing periods of very low turbulence; gap-filling; and partitioning into GPP and R_{eco} (typically using a temperature dependant model of R_{eco} fitted to night time data when GPP is zero). This means that eddy covariance data are not a truly accurate measure of carbon flux, yet they are often treated as though they are a direct measurement. Chamber fluxes are usually considered to be on too small a scale to be a useful validation method for remotely sensed flux estimates, and there are concerns that collar insertion methodology may cause inaccurate results (Heinemeyer et al., 2011). In particular, the short timescale and small area of chamber measurements means that extrapolating to a whole satellite pixel over several months is likely to give results so inaccurate as to be meaningless.

One advantage of satellites with long time series, such as Landsat and MODIS, is that between instrument errors are avoided. Infra-Red Gas Analysers (IRGAs) used in chamber studies and Eddy Covariance towers have advanced greatly in precision over the last decade, meaning that comparison between early and modern chamber or EC studies is difficult. Satellites with long time series do not have this problem because the instrument is the same. Satellites also avoid the operator error which can occur between researchers using different protocols for their chamber or EC studies. The frequency of measurements can increase precision in satellite data compared to chamber studies, particularly for satellites with a frequent return interval.

Future studies intending to use RS data should consider the resolution and coverage of available RS data when designing their ground-validation methodology. In particular, footprint size and coverage in relation to EC towers, and sampling locations and frequency in relation to chamber studies, should be decided with regard to the RS data. One potential solution to the different coverage of chamber, EC and RS data is to scale fluxes using proportional cover (Forbrich et al., 2011; Marushchak et al., 2013). This can be done in terms of microtopography by considering the proportion of the measured area comprising of hummocks, hollows and lawns (see Fig. 2) or in terms of variation in vegetation species. Issues to consider when attempting proportional cover corrections include the time and access needed to identify features or vegetation over the entire area of the EC footprint or satellite pixel. Enough measurements should be taken to allow a reliable average for each identified feature type or vegetation species. The proportional cover can be determined by surveying the entire footprint area, possibly using aerial photography. It is also important to have ground validation data for all seasons, as different vegetation species can have a proportionally very different contribution to fluxes at different times of the year.

5. Potential future work

The previous section (Section 4) has highlighted a number of challenging issues which must be addressed when RS methods are applied to peatland environments. More work is clearly needed in overcoming these challenges, particularly in separating the signal of vascular plants from mosses, and in considering the problems of heterogeneous microtopography and peatland types (see Section 4). This section, however, discusses some of the largest gaps this review has identified in the literature which need to be addressed in future in order to improve remotely sensed estimates of carbon fluxes over peatlands.

The area of remote sensing carbon flux estimation over all ecosystems is dynamic and wide ranging, with many different models and methodologies being developed. The problem with many of these studies, however, is that they are too narrow for comparison. They consider one particular site in one particular ecosystem, and develop a remote sensing model which gives good results compared to the flux measuring method on the ground (most often EC). Even studies which look at multiple sites and attempt to create a global model often focus on a narrow range of only four or five ecosystem types. Peatlands and their huge variety of types are almost never included as a separate category in remote sensing models of carbon flux, and as such are certain to be over or under-estimated. More cohesive studies are therefore needed, which not only look at peatland carbon fluxes across sites and countries, but also which link peatland flux models to those developed in other ecosystems.

Roulet et al. (2007) point out that the peatland carbon cycle is complex and includes many components, some of which are under-studied. Peatland studies using remote sensing have so far focused almost entirely on estimating GPP, and there is a need for more work on the potential of remote sensing for estimating respiration fluxes. One major challenge when using current models of R_{eco} over peatland environments is that they are designed for use on well-drained soils, and so

do not include the concept that water saturation may decrease soil respiration. In carbon peatland studies using field measurements, NEE calculations dominate. There are few studies that combine NEE with CH_4 and DOC, and there is very little work combining these using remote sensing (Sturtevant and Oechel, 2013; Watts et al., 2014).

Considering the range of GPP models discussed in Section 2.2.3, it is evident that LUE-based models are still the dominant method for using RS to assess the carbon uptake of ecosystems. Most studies agree that the MOD17 product is a poor estimate for peatland GPP, most likely because the LUE modifiers are based on a look-up table with no specific peatland category. NDVI and EVI are both widely used as proxies for *f*PAR, and studies over peatland have given good results using one or the other of these indices. More work is needed, however, to determine which is the most effective proxy, particularly when combined with other model factors. Narrow-band indices such as PRI should also be considered in future studies, particularly with the operation of new narrow-band satellite sensors such as EnMAP.

In both peatland and other ecosystem studies, temperature and water stress have been shown to be useful modifiers of LUE and to improve the model results. There is still much debate about the best indices to use, however, particularly for water stress which is an essential consideration in peatlands, given their semi-permanent saturation. Future studies should seek to determine which water indices are best able to capture the entire range of water contents experienced within peatland landscapes.

An interesting avenue of future work would be to consider combining visible and NIR data with RS data from other sources such as InSAR. The combination of texture, elevation and colour changes has the potential to inform a future generation of peatland models.

There is a need for more long-term studies on peatland in order to inform the temporal variability that should be expected of model outputs, and the inputs that are most influential in longer-term peatland carbon flux variations (Marushchak et al., 2013; Helfter et al., 2015; Strachan et al., 2016). Some satellites (e.g. Landsat) have long data archives, which could be extremely useful in historical studies of peatland carbon flux, but only if the models used are validated under appropriate conditions. Carbon fluxes are known to vary greatly between years at the same site, and it is possible for a peatland to be a carbon source one year and a sink the next (Silvola et al., 1996; Lafleur et al., 2003; Roulet et al., 2007; Yu, 2012). For example, Roulet et al. (2007) monitored a bog in Canada for six years, with the lowest annual NEE (greatest sink) during the period of -112 g CO_2/m^2 and the highest (smallest sink) of -2 g CO_2/m^2. Many field studies only report on one growing season and exclude winter fluxes altogether, therefore potentially underestimating annual R_{eco} (Roulet et al., 2007; Sturtevant and Oechel, 2013). It is also important to repeat studies across several different types of peatland, as it cannot be assumed that areas with different characteristics will respond in a similar manner to environmental changes (Lund et al., 2010; Kross et al., 2016). Remote sensing has the potential to easily estimate carbon fluxes over large areas and long periods of time and could therefore fill a gap in the literature of long-term carbon flux studies over peatlands - but it is important to have reliable models first, and to continue to validate models appropriately.

As restoration of peatland offers the potential to increase carbon sequestration (Silvola et al., 1996; Urbanová et al., 2013; Beetz et al., 2013), it is important to increase understanding of how rewetting affects peatland carbon fluxes in the long term (Bussell et al., 2010). Modelling driven by remote sensing data could be a useful approach for large-scale monitoring of peatland restoration schemes, but more work is needed on whether RS data can adequately detect changes in peatland carbon fluxes that are due to restoration processes. We are currently unaware of any published studies utilising remotely sensed data to examine the effects of restoration on carbon fluxes from peatlands. Restoration is generally accepted to improve carbon uptake in comparison to drained and degraded sites, even if the resulting carbon balance is still net emitting or near neutral (Beetz et al., 2013). However, several studies have shown that rewetting is more effective on some peatland sites than others, and there may be some areas which can be improved but never fully restored to a near-natural condition (Basiliko et al., 2007; Clark et al., 2010; Worrall et al., 2011). It is therefore important to have more long term (5 years plus) studies on restoration of different peatland types, in an attempt to characterise what makes a peatland more or less likely to be producing reduced carbon emissions through restoration, and to analyse which restoration methods are the most successful (Bain et al., 2011). Many restoration programmes on Northern peatlands are still in their early stages, and it will be important to continue monitoring on longer timescales of several decades. This is an area of future work into which RS could be usefully integrated.

6. Conclusions

This critical review provides clear evidence for the potential of using RS methods in Northern peat bog carbon flux estimations as well as in other peatlands around the world. The review also highlights a number of cautionary issues which must be accommodated when using RS methods in a peatland habitat, and it identifies a number of challenges which have yet to be adequately tackled.

Some researchers have already applied GPP models to peatland ecosystems, and some have focused on the effectiveness of specific aspects, such as the correlation of vegetation indices with peatland dynamics. The studies considered in this review suggest that the best RS GPP model for peatlands is likely to include either NDVI or EVI, and to have both temperature and water modifiers of LUE. There are many ways of measuring water stress using RS data, and the studies in this review suggest that visible and NIR wavelengths produce potentially usable estimates of peatland water through indices such as the LSWI, WI and fWBI. The best model is therefore likely to be based on visible and NIR wavelengths which are readily available from several satellite sensors already in operation, although spatial resolution will be improved by newer satellites with finer sensor capabilities.

Respiration is a harder problem to solve in RS models of peatland carbon fluxes. Different studies have modelled respiration in very different ways, and there is as yet no commonly used model structure as there is with the LUE model for GPP. The studies considered in this review suggest that respiration (both Ra and Rh) is sensitive to temperature and to productivity/biomass. In addition, soil respiration is concluded to be sensitive to soil water content. Water is especially important in peatlands, which may have the opposite response to most ecosystems – increasing soil respiration with lower than normal water levels.

Many of the problems encountered when applying RS models of carbon fluxes to peatlands are the same as for any other ecosystem: satellite issues such as atmospheric scattering and geocorrection and ground validation issues with the estimation of fluxes from methods such as EC. However, other concerns are unique to peatland environments, such as the spectral and height differences between vascular and non-vascular vegetation types, and the microscale heterogeneity of many peatlands. More work is therefore needed into the upscaling of fluxes from a repeat mosaic environment, and into the potential of having a model which splits its parameterisation between vascular and non-vascular vegetation.

This review suggests that there is a need for multi-disciplinary studies across several peatland sites over several years using RS. Remote sensing models, particularly those for GPP, are now attaining levels of confidence where they could be considered plausible additions to the suite of methods used to measure carbon exchange in peat bog sites. Of particular interest would be studies that explore the potential use of RS in the construction of total carbon budgets, including GPP, R_{eco}, CH_4 and DOC. There is, however, so far little published information in the peer-reviewed literature from sites which have been subject to restoration management. This dearth of information is surprising, given

the high profile now afforded peatland ecosystems within decision-making circles around the world and the scale of resources devoted to such restoration in order to stem carbon losses and restore long-term carbon storage.

Acknowledgements

Thanks to RSPB Forsinard for site access and sampling permission. Thanks to Kevin White for help with the Ger3700 spectrometer. We are grateful to the Natural Environment Research Council Airborne Research Facility for use of the image in figure 3. Thanks to Matt Aitkenhead for proof reading and comments and to the two anonymous reviewers for their helpful critiques.

Funding

Kirsten Lees is part funded by a studentship from The James Hutton Institute, and part funded by the Natural Environment Research Council (NERC) SCENARIO DTP (Grant number: NE/L002566/1). Tristan Quaife is funded by the NERC National Centre for Earth Observation (NCEO). Myroslava Khomik and Rebekka Artz are funded by The Scottish Government Strategic Research Programme.

References

Anderson, M.C., Norman, J.M., Kustasa, W.P., Houborg, R., Starks, P.J., Agam, N., 2008. A thermal-based remote sensing technique for routine mapping of land-surface carbon, water and energy fluxes from field to regional scales. Remote Sens. Environ. 112 (12), 4227–4241.

Anderson, K., Bennie, J.J., Milton, E.J., Hughes, P.D.M., Lindsay, R., Meade, R., 2009. Combining LiDAR and IKONOS data for eco-hydrological classification of an ombrotrophic peatland. J. Environ. Qual. 39 (1):260–273. https://doi.org/10.2134/jeq2009.0093.

Bain, C.G., Bonn, A., Stoneman, R., Chapman, S., Coupar, A., Evans, M., Gearey, B., Howat, M., Joosten, H., Keenleyside, C., Labadz, J., Lindsay, R., Littlewood, N., Lunt, P., Millder, C.J., Moxy, A., Orr, H., Reed, M., Smith, P., Swales, V., Thompson, D.B.A., Thompson, P.S., Van de Noort, R., Wilson, J.D., Worrall, F., 2011. IUCN UK Commission of Inquiry on Peatlands. IUCN UK Peatland Programme, Edinburgh.

Balzarolo, M., Vicca, S., Nguy-Robertson, A.L., Bonal, D., Elbers, J.A., Fu, Y.H., Grünwald, T., Horemans, J.A., Papale, D., Peñuelas, J., Suyker, A., Veroustraete, F., 2016. Matching the phenology of net ecosystem exchange and vegetation indices estimated with MODIS and FLUXNET in-situ observations. Remote Sens. Environ. 174 (1), 290–300.

Baranoski, G., Rokne, J., 2005. A practical approach for estimating the red edge position of plant leaf reflectance. Int. J. Remote Sens. 26 (3), 503–521.

Basiliko, N., Blodau, C., Roehm, C., Bengtson, P., Moore, T.R., 2007. Regulation of decomposition and methane dynamics across natural, commercially mined, and restored northern peatlands. Ecosystems 10:1148–1165. https://doi.org/10.1007/s10021-007-9083-2.

Beetz, S., Liebersbach, H., Glatzel, S., Jurasinski, G., Buczko, U., Höper, H., 2013. Effects of land use intensity on the full greenhouse gas balance in an Atlantic peat bog. Biogeosciences 10:1067–1082. https://doi.org/10.5194/bg-10-1067-2013.

Bryant, R.G., Baird, A.J., 2003. The spectral behaviour of Sphagnum canopies under varying hydrological conditions. Geophys. Res. Lett. 30 (3):1134–1138. https://doi.org/10.1029/2002GL016053.

Bubier, J.L., Rock, B.N., Crill, P.M., 1997. Spectral reflectance measurements of boreal wetland and forest mosses. J. Geophys. Res. 102 (D24), 29483–29494.

Bubier, J.L., Bhatia, G., Moore, T., Roulet, N., Lafleur, P., 2003. Spatial and temporal variability in growing-season net ecosystem carbon dioxide exchange at a large peatland in Ontario, Canada. Ecosystems 6, 353–367.

Bussell, J., Jones, D.L., Healey, J.R., Pullin, A., 2010. How do draining and re-wetting affect carbon stores and greenhouse gas fluxes in peatland soils? CEE Review 08-012 (SR49) Available online: Collaboration for Environmental Evidence. www.environmentalevidence.org/SR49.html

Chong, M., Humphreys, E., Moore, T.R., 2012. Microclimatic response to increasing shrub cover and its effect on Sphagnum CO2 exchange in a bog. Ecoscience 19 (1):89–97. https://doi.org/10.2980/19-1-3489.

Christian, B., Joshi, N., Saini, M., Mehta, N., Goroshi, S., Nidamanuri, R.R., Thenkabail, P., Desai, A.R., Krishnayya, N.S.R., 2015. Seasonal variations in phenology and productivity of a tropical dry deciduous forest from MODIS and Hyperion. Agric. For. Meteorol. 214–215, 91–105.

Cigna, F., Sowter, A., 2017. The relationship between intermittent coherence and precision of ISBAS InSAR ground motion velocities: ERS-1/2 case studies in the UK. Remote Sens. Environ. https://doi.org/10.1016/j.rse.2017.05.016.

Clark, J., Gallego-Sala, A., Allott, E., Chapman, S., Farewell, T., Freeman, C., House J, Orr, H., Prentice, I., Smith, P., 2010. Assessing the vulnerability of blanket peat to climate change using an ensemble of statistical bioclimatic envelope models. Clim. Res. 45, 131–150.

Connolly, J., Roulet, N.T., Seaquist, J.W., Holden, N.M., Lafleur, P.M., Humphreys, E.R., Heumann, B.W., Ward, S.M., 2009. Using MODIS derived fPAR with ground based flux tower measurements to derive the light use efficiency for two Canadian peatlands. Biogeosciences 6 (2), 225–234.

Crichton, K.A., Anderson, K., Bennie, J.J., Milton, E.J., 2014. Characterizing peatland carbon balance estimates using freely available Landsat ETM + data. Ecohydrology 493–503.

Dash, J., Curran, P.J., 2004. The MERIS terrestrial chlorophyll index. Int. J. Remote Sens. 25 (23):5403–5413. https://doi.org/10.1080/0143116042000274015.

DigitalGlobe, 2016. About our constellation. https://www.digitalglobe.com/about/our-constellation, Accessed date: 28 October 2016.

Dinsmore, K.J., Skiba, U.M., Billett, M.F., Rees, R.M., 2009. Effect of water table on greenhouse gas emissions from peatland mesocosms. Plant Soil 318, 229–242.

Dong, J., Xiao, X., Wagle, P., Zhang, G., Zhou, Y., Jin, C., Torn, M.S., Meyers, T.P., Suyker, A.E., Wang, J., Yan, H., Biradar, C., Moor, B., 2015. Comparison of four EVI-based models for estimating gross primary production of maize and soybean croplands and tallgrass prairie under severe drought. Remote Sens. Environ. 162, 154–168.

Drolet, G.G., Huemmrich, K.F., Hall, F.G., Middleton, E.M., Black, T.A., Barr, A.G., Margolis, H.A., 2005. A MODIS-derived photochemical reflectance index to detect inter-annual variations in the photosynthetic light-use efficiency of a boreal deciduous forest. Remote Sens. Environ. 98 (2), 212–224.

EnMAP, 2016. EnMAP – hyperspectral imager. http://www.enmap.org, Accessed date: 28 October 2016.

ESA, 2015. No 42–2015: FLEX mission to be next ESA earth explorer. http://www.esa.int/For_Media/Press_Releases/FLEX_mission_to_be_next_ESA_Earth_Explorer, Accessed date: 28 October 2016.

ESA, 2016. ESA EO missions. https://earth.esa.int/web/guest/missions/esa-eo-missions, Accessed date: 28 October 2016.

ESA, 2017. MERIS. Available online. https://earth.esa.int/web/guest/missions/esa-operational-eo-missions/envisat/instruments/meris, Accessed date: 4 April 2017.

Fleischer, E., Khashimov, I., Hölzel, N., Klemm, O., 2016. Carbon exchange fluxes over peatlands in Western Siberia: possible feedback between land-use change and climate change. Sci. Total Environ. 545–546, 424–433.

Forbrich, I., Kutzbach, L., Wille, C., Becker, T., Wu, J., Wilmking, M., 2011. Cross-evaluation of measurements of peatland methane emissions on microform and ecosystem scales using high resolution land cover classification and source weight modelling. Agric. For. Meteorol. 151, 864–874.

Frankenberg, C., O'Dell, C., Berry, J., Guanter, L., Joiner, J., Köhler, P., Pollock, R., Taylor, T.E., 2014. Prospects for chlorophyll fluorescence remote sensing from the orbiting carbon observatory-2. Remote Sens. Environ. 147, 1–12.

Frolking, S.E., Bubier, J.L., Moore, T.R., Ball, T., Bellisario, L.M., Bhardwaj, A., Carroll, P., Crill, P.M., Lafleur, P.M., McCaughey, H., Roulet, N.T., Suyker, A.E., Verrna, S.B., Waddington, M., Whiting, G.J., 1998. Relationship between ecosystem productivity and photosynthetically active radiation for northern peatlands. Glob. Biogeochem. Cycles 12 (1), 115–126.

Gamon, J.A., Peñuelas, J., Field, C.B., 1992. A narrow-waveband spectral index that tracks diurnal changes in photosynthetic efficiency. Remote Sens. Environ. 41, 35–44.

Gao, B.C., 1996. NDWI a normalized difference water index for remote sensing of vegetation liquid water from space. Remote Sens. Environ. 58, 257–266.

Gao, F., Masek, J., Schwaller, M., Hall, F., 2006. On the blending of the Landsat and MODIS surface reflectance: predict daily Landsat surface reflectance. IEEE Trans. Geosci. Remote Sens. 44 (8), 2207–2218.

Gao, Y., Yu, G., Li, S., Yan, H., Zhu, X., Wang, Q., Shi, P., Zhao, L., Li, Y., Zhang, F., Wang, Y., Zhang, J., 2015. Remote sensing model to estimate ecosystem respiration in Northern China and the Tibetan Plateau. Ecosyst. Model. 304, 34–43.

Garbulsky, M.F., Peñuelas, J., Gamon, J., Inoue, Y., Filella, I., 2011. The Photochemical Reflectance Index (PRI) and the remote sensing of leaf, canopy and ecosystem radiation use efficiencies; a review and meta-analysis. Remote Sens. Environ. 115, 281–297.

Garrigues, S., Lacaze, R., Baret, F., Morisette, J.T., Weiss, M., Nickeson, J.E., Fernandes, R., Plummer, S., Shabanov, N.V., Myneni, R.B., Knyazikhin, Y., Yang, W., 2008. Validation and intercomparison of global Leaf Area Index products derived from remote sensing data. J. Geophys. Res.:113 https://doi.org/10.1029/2007JG000635.

Gitelson, A.A., Peng, Y., Masek, J.G., Rundquist, D.C., Verma, S., Suyker, A., Baker, J.M., Hatfield, J.L., Meyers, T., 2012. Remote estimation of crop gross primary production with Landsat data. Remote Sens. Environ. 121, 404–414.

Goerner, A., Reichstein, M., Tomelleri, E., Hanan, N., Rambal, S., Papale, D., Dragoni, D., Schmullius, C., 2011. Remote sensing of ecosystem light use efficiency with MODIS-based PRI. Biogeosciences 8 (1), 189–202.

Gorham, E., 1991. Northern peatlands – role in the carbon cycle and probable responses to climatic warming. Ecol. Appl. 1 (2), 182–195.

Grace, J., Nichol, C., Disney, M., Lewis, P., Quaife, T., Bowyer, P., 2007. Can we measure terrestrial photosynthesis from space directly, using spectral reflectance and fluorescence? Glob. Chang. Biol. 13 (7), 1484–1497.

Guanter, L., Alonso, L., Gómez-Chova, L., Amorós-López, J., Vila, J., Moreno, J., 2007. Estimation of solar-induced vegetation fluorescence from space measurements. Geophys. Res. Lett. 34, 8.

Harris, A., 2008. Spectral reflectance and photosynthetic properties of Sphagnum mosses exposed to progressive drought. Ecohydrology 1 (1):35–42. https://doi.org/10.1002/eco.5.

Harris, A., Bryant, R.G., 2009. A multi-scale remote sensing approach for monitoring northern peatland hydrology: present possibilities and future challenges. J. Environ. Manag. 90 (7), 2178–2188.

Harris, A., Dash, J., 2011. A new approach for estimating northern peatland gross primary productivity using a satellite-sensor-derived chlorophyll index. J. Geophys. Res. 116, G4.

Harris, A., Bryant, R.G., Baird, A.J., 2005. Detecting near-surface moisture stress in Sphagnum spp. Remote Sens. Environ. 97 (3):371–381. https://doi.org/10.1016/j.rse.2005.05.001.

Harris, A., Bryant, R.G., Baird, A.J., 2006. Mapping effects of water stress on Sphagnum: preliminary observations using airborne remote sensing. Remote Sens. Environ. 100:363–378. https://doi.org/10.1016/j.rse.2005.10.024.

Harris, A., Gamon, J.A., Pastorello, G.Z., Wong, C.Y.S., 2014. Retrieval of the photochemical reflectance index for assessing xanthophyll cycle activity: a comparison of near-surface optical sensors. Biogeosciences 11, 6277–6292.

Heinemeyer, A., Di Bene, C., Lloyd, A., Tortorella, D., Baxter, R., Huntley, B., Gelsomino, A., Ineson, P., 2011. Soil respiration: implications of the plant-soil continuum and respiration chamber collar-insertion depth on measurement and modelling of soil CO_2 efflux rates in three ecosystems. Eur. J. Soil Sci. 62, 82–94.

Heinsch, F.A., Zhao, M., Running, S.W., Kimball, J.S., Nemani, R.R., Davis, K.J., Bolstad, P.V., Cook, B.D., Desai, A.R., Ricciuto, D.M., Law, B.E., Oechel, W.C., Kwon, H., Luo, H., Wofsy, S.C., Dunn, A.L., Munger, J.W., Baldocchi, D.D., Liukang, X., Hollinger, D.Y., Richardson, A.D., Stoy, P.C., MBS, Siqueira, Monson, R.K., Burns, S.P., Flanagan, L.B., 2006. Evaluation of remote sensing based terrestrial productivity from MODIS using regional tower eddy flux network observations. IEEE Trans. Geosci. Remote Sens. 1908–1925.

Helfter, C., Campbell, C., Dinsmore, K.J., Drewer, J., Coyle, M., Anderson, M., Skiba, U., Nemitz, E., Billett, M.F., Sutton, M.A., 2015. Drivers of long-term variability in CO_2 net ecosystem exchange in a temperate peatland. Biogeosciences 12, 1799–1811.

Heute, A., Didan, K., Miura, T., Rodriguez, E.P., Gao, X., Ferreira, L.G., 2002. Overview of the radiometric and biophysical performance of the MODIS vegetation indices. Remote Sens. Environ. 83, 195–213.

Hilker, T., Coops, N.C., Wulder, M.A., Black, A., Guy, R.D., 2008. The use of remote sensing in light use efficiency based models of gross primary production: a review of current status and future requirements. Sci. Total Environ. 404 (2–3), 411–423.

Hill, T.C., Quaife, T., Williams, M., 2011. A data assimilation method for using low-resolution Earth observation data in heterogeneous ecosystems. J. Geophys. Res. Atmos. 116, D8.

Hiraishi, T., Krug, T., Boer, R., Gonzalez, S., Penman, J., Sturgiss, R., Zhakata, W., Tanabe, K., Srivastava, N., 2013. 2013 revised supplementary methods and good practice guidance arising from the Kyoto protocol: overview. Available online:. http://www.ipcc-nggip.iges.or.jp/public/kpsg/pdf/KP_Separate_files/KP_Overview.pdf, Accessed date: 9 February 2017.

Huemmrich, K.F., Gamon, J.A., Tweedie, C.E., Oberbauer, S.F., Kinoshita, G., Houston, S., Kuchy, A., Hollister, R.D., Kwon, H., Mano, M., Harazono, Y., Webber, P.J., Oechel, W.C., 2010. Remote sensing of tundra gross ecosystem productivity and light use efficiency under varying temperature and moisture conditions. Remote Sens. Environ. 114 (3), 481–489.

Humphreys, E.R., Lafleur, P.M., Flanagan, L.B., Hedstrom, N., Syed, K.H., Glenn, A.J., Granger, R., 2006. Summer carbon dioxide and water vapor fluxes across a range of northern peatlands. J. Geophys. Res. Biol. 111, G04011. https://doi.org/10.1029/2005JG000111.

IPCC, 2014. In: Hiraishi, T., Krug, T., Tanabe, K., Srivastava, N., Baasansuren, J., Fukuda, M., Troxler, T.G. (Eds.), 2013 Supplement to the 2006 IPCC Guidelines for National Greenhouse Gas Inventories: Wetlands. IPCC, Switzerland.

Jägermeyr, J., Gerten, D., Lucht, W., Hostert, P., Miglavacca, M., Nemani, R., 2014. A high-resolution approach to estimating ecosystem respiration at continental scales using operational satellite data. Glob. Chang. Biol. 20 (4), 1191–1210.

Kasischke, E.S., Bourgeau-Chavez, L.L., Rober, A.R., Wyatt, K.H., Waddington, J.M., Turetsky, M.R., 2009. Effects of soil moisture and water depth on ERS SAR backscatter measurements from an Alaskan wetland complex. Remote Sens. Environ. 113, 1868–1873.

Kraft, S., Del Bello, U., Harnisch, B., Bouvet, M., Drusch, M., Bezy, J.L., 2012. Fluorescence imaging spectrometer concepts for the earth explorer mission candidate FLEX. http://esaconferencebureau.com/custom/icso/2012/papers/FP_ICSO-081.pdf, Accessed date: 27 January 2017.

Kross, A., Seaquist, J.W., Roulet, N.T., Fernandes, R., Sonnentag, O., 2013. Estimating carbon dioxide exchange rates at contrasting northern peatlands using MODIS satellite data. Remote Sens. Environ. 137, 234–243.

Kross, A., Seaquist, J.W., Roulet, N.T., 2016. Light use efficiency of peatlands: variability and suitability for modeling ecosystem production. Remote Sens. Environ. 183:239–249. https://doi.org/10.1016/j.rse.2016.05.004.

Lafleur, P.M., Roulet, N.T., Bubier, J.L., Frolking, S., Moore, T.R., 2003. Interannual variability in the peatland-atmosphere carbon dioxide exchange at an ombrotrophic bog. Glob. Biogeochem. Cycles 17 (2):1036. https://doi.org/10.1029/2002GB001983.

Landsberg, J.J., Waring, R.H., 1997. A generalised model of forest productivity using simplified concepts of radiation-use efficiency, carbon balance and partitioning. For. Ecol. Manag. 95 (3):209–228. https://doi.org/10.1016/S0378-1127(97)00026-1.

Letendre, J., Poulin, M., Rochefort, L., 2008. Sensitivity of spectral indices to CO_2 fluxes for several plant communities in a Sphagnum-dominated peatland. Can. J. Remote. Sens. 34 (2), 414–S425.

Levy, P., Gray, A., 2015. Greenhouse gas balance of a semi-natural peatbog in northern Scotland. Environ. Res. Lett. 10.

Limpens, J., Berendse, F., Blodau, C., Canadell, J.G., Freeman, C., Holden, J., Roulet, N., Rydin, H., Schaepman-Strub, G., 2008. Peatlands and the carbon cycle: from local processes to global implications – a synthesis. Biogeosciences 5, 1475–1491.

Lindsay, R., 2010. Peatbogs and carbon: a critical synthesis to inform policy development in oceanic peat bog conservation and restoration in the context of climate change. RSPB Scotland. Available online:. http://roar.uel.ac.uk/1144/1/Lindsay%2C%20R.%20%282010%29%20Peatbogs%20%26%20Carbon.pdf, Accessed date: 4 July 2017.

Lindsay, R.A., Rigall, J., Durd, F., 1985. The use of small-scale surface patterns in the classification of British Peatlands. Aquil. Ser. Bot. 21, 67–79.

Lloyd, J., Taylor, J.A., 1994. On the temperature dependence of soil respiration. Funct. Ecol. 8, 315–323.

Lund, M., Lafleur, P., Roulet, N., Lindroth, A., Christensen, T., Aurela, M., Chojnicki, B., Flanagan, L., Humphreys, E., Laurila, T., Oechel, W., Olejnik, J., Rinne, J., Schubert, P., Nilsson, M., 2010. Variability in exchange of CO_2 across 12 northern peatland and tundra sites. Glob. Chang. Biol. 16 (9), 2436–2448.

Lund, M., Christensen, T.R., Lindroth, A., Schubert, P., 2012. Effects of drought conditions on the carbon dioxide dynamics in a temperate peatland. Environ. Res. Lett. 7.

Malenovsky, Z., Turnbull, J., Lucieer, A., Robisnon, S., 2015. Antarctic moss stress assessment based on chlorophyll content and leaf density retrieved from imaging spectroscopy data. New Phytol. 208, 608–624.

Marushchak, M.E., Kiepe, I., Biasi, C., Elsakov, V., Friborg, T., Johansson, T., Soegaard, H., Virtanen, T., Martikained, P.J., 2013. Carbon dioxide balance of subarctic tundra from plot to regional scales. Biogeosciences 10, 437–452.

McMorrow, J.M., Cutler, M.E.J., Evans, M.G., AlRoichdi, A., 2004. Hyperspectral indices for characterizing upland peat composition. Int. J. Remote Sens. 25 (2):313–325. https://doi.org/10.1080/0143116031000117065.

Meingast, K.M., Falkowski, M.J., Kane, E.S., Potvin, L.R., Benscoter, B.W., Smith, A.M.S., Bourgeau-Chavez, L.L., Miller, M.E., 2014. Spectral detection of near-surface moisture content and water-table position in northern peatland ecosystems. Remote Sens. Environ. 152, 536–546.

Meroni, M., Rossini, M., Guanter, L., Alonso, L., Rascher, U., Colombo, R., Moreno, J., 2009. Remote sensing of solar-induced chlorophyll fluorescence: review of methods and applications. Remote Sens. Environ. 113 (10), 2037–2051.

Min, Q., 2005. Impacts of aerosols and clouds on forest-atmosphere carbon exchange. J. Geophys. Res. 110:d6. https://doi.org/10.1029/2004JD004858.

Monteith, J.L., 1977. Climate and the efficiency of crop production in Britain. Philos. Trans. R. Soc. Lond. 281, 277–294.

NASA, 2010. Artist's rendering of Aqua. https://earthobservatory.nasa.gov/Features/Water/page4.php, Accessed date: 7 September 2017.

NASA, 2016a. MODIS – Moderate Resolution Imaging Spectroradiometer. available at:. https://modis.gsfc.nasa.gov, Accessed date: 28 October 2016.

NASA, 2016b. Orbiting carbon observatory 2. http://www.nasa.gov/mission_pages/oco2/index.html, Accessed date: 28 October 2016.

NASA, 2016c. HysplRl mission study. https://hyspiri.jpl.nasa.gov, Accessed date: 28 October 2016.

NERC, 2016. Airborne research & survey facility. http://arsf.nerc.ac.uk, Accessed date: 5 April 2017.

NIES, 2016. GOSAT project – greenhouse gases observing satellite. http://www.gosat.nies.go.jp/en/, Accessed date: 28 October 2016.

Nilsson, M., Sagerfors, J., Buffam, I., Laudon, H., Eriksson, T., Grelle, A., Klemedtsson, L., Weslien, P., Lindroth, A., 2008. Contemporary carbon accumulation in a boreal oligotrophic minerogenic mire—a significant sink after accounting for all C-fluxes. Glob. Chang. Biol. 14 (10):2317–2332. https://doi.org/10.1111/j.1365-2486.2008.01654.x.

Olofsson, P., Lagergren, F., Lindroth, A., Lindström, J., Klemedtsson, L., Kutsch, W., Eklundh, L., 2008. Towards operational remote sensing of forest carbon balance across Northern Europe. Biogeosciences 5:817–832. https://doi.org/10.5194/bg-5-817-2008.

Parry, L.E., Chapman, P.J., Palmer, S.M., Wallage, Z.E., Wynnea, H., Holden, J., 2015. The influence of slope and peatland vegetation type on riverine dissolved organic carbon and water colour at different scales. Sci. Total Environ. 527–528:530–539. https://doi.org/10.1016/j.scitotenv.2015.03.036.

Peñuelas, J., Filella, I., Gamon, J.A., 1995. Assessment of photosynthetic radiation-use efficiency with spectral reflectance. New Phytol. 131, 291–296.

Peñuelas, J., Pinol, J., Ogaya, R., Filella, I., 1997. Estimation of plant water concentration by the reflectance Water Index WI (R900/R970). Int. J. Remote Sens. 18 (13):2869–2875. https://doi.org/10.1080/014311697217396.

Peñuelas, J., Garbulsky, M.F., Filella, I., 2011. Photochemical reflectance index (PRI) and remote sensing of plant CO_2 uptake. New Phytol. 191 (3), 596–599.

Pfeifer, M., Disney, M., Quaife, T., Marchant, R., 2012. Terrestrial ecosystems from space: a review of earth observation products for macroecology applications. Glob. Ecol. Biogeogr. 21 (6), 603–624.

Potter, C.S., Randerson, J.T., Field, C.B., Matson, P.A., Vitousek, P.M., Mooney, H.A., Klooster, S.A., 1993. Terrestrial ecosystem production: a process model based on global satellite and surface data. Glob. Biogeochem. Cycles 7 (4), 811–841.

Prince, S.D., Goward, S.N., 1995. Global primary production: a remote sensing approach. J. Biogeogr. 22 (4/5), 815–835.

Rahman, A.F., Sims, D.A., Cordova, V.D., El-Masri, B.Z., 2005. Potential of MODIS EVI and surface temperature for directly estimating per-pixel ecosystem C fluxes. Geophys. Res. Lett. 32, 19.

Reichstein, M., Rey, A., Freibauer, A., Tenhunen, J., Valentini, R., Banza, J., Casals, P., Cheng, Y., Grünsweig, J.M., Irvine, J., Joffre, R., Law, B.E., Loustau, D., Miglietta, F., Oechel, W., Ourcival, J.M., Pereira, J.S., Peressotti, A., Ponti, F., Qi, Y., Rambal, S., Rayment, M., Romanya, J., Rossi, F., Tedeschi, V., Tirone, G., Xu, M., Yakir, D., 2003. Modeling temporal and large-scale spatial variability of soil respiration from soil water availability, temperature and vegetation productivity indices. Glob. Biogeochem. Cycles 17, 4.

Rossini, M., Cogliati, S., Meroni, M., Migliavacca, M., Galvagno, M., Busetto, L., Cremonese, E., Julitta, T., Siniscalco, C., Morra di Cella, U., Colombo, R., 2012. Remote sensing-based estimation of gross primary production in a subalpine grassland. Biogeosciences 9, 2565–2584.

Roulet, N.T., Lafleur, P.M., Richard, P.J.H., Moore, T.R., Humphreys, E.R., Bubier, J., 2007. Contemporary carbon balance and late Holocene carbon accumulation in a northern peatland. Glob. Chang. Biol. 13, 397–411.

Running, S., Zhao, M., 2015. User's guide - daily GPP and annual NPP (MOD17A2/A3) products - NASA Earth observing system MODIS land algorithm. Available online:. http://www.ntsg.umt.edu/sites/ntsg.umt.edu/files/modis/MOD17UsersGuide2015_v3.pdf, Accessed date: 28 October 2016.

Running, S.W., Nemani, R.R., Heinsch, F.A., Zhao, M., Reeves, M., Hashimoto, H., 2004. A continuous satellite-derived measure of global terrestrial primary production. Bioscience 54, 547–560.

Schubert, P., Eklundh, L., Lund, M., Nilsson, M., 2010. 1189 Estimating northern peatland CO_2 exchange from MODIS time series data. Remote Sens. Environ. 114, 1178–1189.

Shurpali, N.J., Verma, S.B., Kim, J., Arkebauer, T.J., 1995. Carbon dioxide exchange in a peatland ecosystem. J. Geophys. Res. 100:14319–14326. https://doi.org/10.1029/95JD01227.

Silvola, J., Alm, J., Ahlholm, U., Nykanen, H., Martikainen, P.J., 1996. Fluxes from peat in boreal mires under varying temperature and moisture conditions. J. Ecol. 84 (2), 219–228.
Sims, D., Rahman, A., Cordova, V., El-Masri, B., Baldocchi, D., Bolstad, P., Flanagan, L., Goldstein, A., Hollinger, D., Misson, L., Monson, R., Oechel, W., Schmid, H., Wofsy, S., Xu, L., 2008. A new model of gross primary productivity for North American ecosystems based solely on the enhanced vegetation index and land surface temperature from MODIS. Remote Sens. Environ. 112, 1633–1646.
Stoy, P.C., Quaife, T., 2015. Probabilistic downscaling of remote sensing data with applications for multi-scale biogeochemical flux modeling. PLoS One 10 (6), e0128935. https://doi.org/10.1371/journal.pone.0128935.
Strachan, I.B., Pattey, E., Boisvert, J.B., 2002. Impact of nitrogen and environmental conditions on corn as detected by hyperspectral reflectance. Remote Sens. Environ. 80 (2), 213–224.
Strachan, I.B., Pelletier, L., Bonneville, C., 2016. Inter-annual variability in water table depth controls net ecosystem carbon dioxide exchange in a boreal bog. Biogeochemistry 127:99–111. https://doi.org/10.1007/s10533-015-0170-8.
Sturtevant, C.S., Oechel, W.C., 2013. Spatial variation in landscape-level CO_2 and CH4 fluxes from arctic coastal tundra: influence from vegetation, wetness, and the thaw lake cycle. Glob. Chang. Biol. 19 (9), 2853–2866.
Tagesson, T., Mastepanov, M., Mölder, M., Tamstorf, M.P., Eklundh, L., Smith, B., Sigsgaard, C., Lund, M., Ekberg, A., Falk, J.M., Friborg, T., Christensen, T.R., Ström, L., 2013. Modelling of growing season methane fluxes in a high-Arctic wet tundra ecosystem 1997–2010 using in situ and high-resolution satellite data. Tellus Ser. B Chem. Phys. Meteorol. 6:19722. https://doi.org/10.3402/tellusb.v65i0.19722.
Tan, K.P., Devi, K., Cracknell, A.P., 2012. A review of remote sensing based productivity models and their suitability for studying oil palm productivity in tropical regions. Prog. Phys. Geogr. 36 (5), 655–679.
Thomas, V., Treitz, P., Jelinskia, D., Miller, J., Lafleur, P., McCaughey, J.M., 2003. Image classification of a northern peatland complex using spectral and plant community data. Remote Sens. Environ. 84 (1):83–99. https://doi.org/10.1016/S0034-4257(02)00099-8.
Turner, D.P., Ritts, W.D., Styles, J.M., Yang, Z., Cohen, W.B., Law, B.E., Thornton, P.E., 2006. A diagnostic carbon flux model to monitor the effects of disturbance and interannual variation in climate on regional NEP. Tellus 58B, 476–490.
Turner, T.E., Billett, M.F., Baird, A.J., Chapman, P.J., Dinsmore, K.J., Holden, J., 2016. Regional variation in the biogeochemical and physical characteristics of natural peatland pools. Sci. Total Environ. 545–546, 84–94.
Urbanová, Z., Picek, T., Tuittila, E.S., 2013. Sensitivity of carbon gas fluxes to weather variability on pristine, drained and rewetted temperate bogs. Mires Peat 11 (4), 1–14.
USGS, 2011. Hyperion. https://eo1.usgs.gov/sensors/hyperion, Accessed date: 28 October 2016.
USGS, 2016. Landsat missions. http://landsat.usgs.gov, Accessed date: 28 October 2016.
Van Gaalen, K.E., Flanagan, L.B., Peddle, D.R., 2007. Photosynthesis, chlorophyll fluorescence and spectral reflectance in Sphagnum moss at varying water contents. Ecophysiol. Oecol. 153 (1), 19–28.
Van Wittenberghe, S., Alonso, L., Verrelst, J., Moreno, J., Samson, R., 2015. Bidirectional sun-induced chlorophyll fluorescence emission is influenced by leaf structure and light scattering properties — a bottom-up approach. Remote Sens. Environ. 158, 169–179.
Verma, M., Friedl, M.A., Law, B.E., Bonal, D., Kiely, G., Black, T.A., Wohlfahrt, G., Moors, E.J., Montagnani, L., Marcolla, B., Toscano, P., Varlagin, A., Roupsard, O., Cescatti, A., Arain, M.A., D'Odorico, P., 2015. Improving the performance of remote sensing models for capturing intra- and inter-annual variations in daily GPP: an analysis using global FLUXNET tower data. Agric. For. Meteorol. 214–215, 416–429.
Vermote, E.F., Tanre, D., Deuze, J.L., Herman, M., Morcrette, J.J., 1997. Second simulation of the satellite signal in the solar spectrum, 6S: an overview. IEEE Trans. Geosci. Remote Sens. 35 (3), 675–686.
Vogelmann, J.E., Moss, D.M., 1993. Spectral reflectance measurements in the genus Sphagnum. Remote Sens. Environ. 45, 273–279.
Vourlitis, G.L., Verfaillie, J., Oechel, W.C., Hope, A., Stow, D., Engestrom, R., 2003. Spatial variation in regional CO_2 exchange for the Kuparuk River Basin, Alaska over the summer growing season. Glob. Chang. Biol. 9 (6), 930–941.
Waddington, J.M., Price, J.S., 2000. Effect of peatland drainage, harvesting, and restoration on atmospheric water and carbon exchange. Phys. Geogr. 21 (5), 433–451.
Waddington, J.M., Roulet, N.T., 1996. Atmosphere-wetland carbon exchanges: scale dependency of and CH 4 exchange on the developmental topography of a peatland. Glob. Biogeochem. Cycles 10 (2), 233–245.
Walker, J.J., de Beurs, K.M., Wynne, R.H., 2014. Dryland vegetation phenology across an elevation gradient in Arizona, USA, investigated with fused MODIS and Landsat data. Remote Sens. Environ. 144, 85–97.
Walker, T.N., Garnett, M.H., Ward, S.E., Oakley, S., Bardgett, R.D., Ostle, N.J., 2016. Vascular plants promote ancient peatland carbon loss with climate warming. Glob. Chang. Biol. 1880–1889.
Waring, R.H., Running, S.W., 1998. Forest Ecosystems. Academic Press, San Diego, CA.
Watts, J.D., Kimball, J.S., Parmentier, F.J.W., Sachs, T., Rinne, J., Zona, D., Oechel, W., Tagesson, T., Jackowicz-Korcynski, M., Aurela, M., 2014. A Satellite Data Driven Biophysical Modeling Approach for Estimating Northern Peatland and Tundra CO2 and CH4 Fluxes. 11 pp. 1961–1980.
Weston, D.J., Timm, C.M., Walker, A.P., Gu, L., Muchero, W., Schmutz, J., Shaw, A.J., Tuskan, G.A., Warren, J.M., Wullschleger, S.D., 2014. Sphagnum physiology in the context of changing climate: emergent influences of genomics, modelling and host–microbiome interactions on understanding ecosystem function. Plant Cell Environ. 38 (9):1737–1751. https://doi.org/10.1111/pce.12458.
Whiting, G.J., 1994. CO_2 exchange in the Hudson Bay lowlands: community characteristics and multispectral reflectance properties. J. Geophys. Res. 99, 1519–1528.
Worrall, F., Chapman, P., Holden, J., Evans, C., Artz, R., Smith, P., Grayson, R., 2011. A review of current evidence on carbon fluxes and greenhouse gas emissions from UK peatland. JNCC Report. 442.
Wu, C., 2012. Use of a vegetation index model to estimate gross primary production in open grassland. J. Appl. Remote. Sens. 6:1. https://doi.org/10.1117/1.JRS.6.063532.
Wu, C., Gaumont-Guay, D., Black, A., Jassal, R.S., Xua, S., Chen, J.M., Gonsamo, A., 2014. Soil respiration mapped by exclusively use of MODIS data for forest landscapes of Saskatchewan, Canada. ISPRS J. Photogramm. Remote Sens. 94, 80–90.
Xiao, X., Zhang, Q., Braswell, B., Urbanski, S., Boles, S., Wofsy, S., Moore, B., Ojima, D., 2004. Modeling gross primary production of temperate deciduous broadleaf forest using satellite images and climate data. Remote Sens. Environ. 91, 256–270.
Yu, Z.C., 2012. Northern peatland carbon stocks and dynamics: a review. Biogeosciences 9:4071–4085. https://doi.org/10.5194/bg-9-4071-2012.
Yu, Q., Wang, S., Mickler, R.A., Huang, K., Yan, H., Chen, D., Han, S., 2014. Narrowband bioindicator monitoring of temperate forest carbon fluxes in Northeastern China. Remote Sens. 6 (9):8986–9013. https://doi.org/10.3390/rs6098986.
Yuan, W.P., Liu, S., Zhou, G.S., Zhou, G.Y., Tieszen, L.L., Baldocchi, D., Bernhofer, C., Gholz, H., Goldstein, A.H., Goulden, M.L., Hollinger, D.Y., Hu, Y., Law, B.E., Stoy, P.C., Vesala, T., Wofsy, S.C., 2007. Deriving a light use efficiency model from eddy covariance flux data for predicting daily gross primary production across biomes. Agric. For. Meteorol. 143, 189–207.
Yuan, W., Liu, S., Yu, G., Bonnefon, J.M., Chen, J., Davis, K., Desai, A.R., Goldstein, A.H., Gianelle, D., Rossi, F., Suyker, A.E., Verma, S.B., 2010. Global estimates of evapotranspiration and gross primary production based on MODIS and global meteorology data. Remote Sens. Environ. 1416–1431.
Yuan, W., Liu, S., Dong, W., Liang, S., Zhao, S., Chen, J., Xu, W., Li, X., Barr, A., Black, T.A., Yan, W., Goulden, M.L., Kulmala, L., Lindroth, A., Margolis, H.A., Matsuura, Y., Moors, E., van der Molen, M., Ohta, T., Pilegaard, K., Varlagin, A., Vesala, T., 2014. Differentiating moss from higher plants is critical in studying the carbon cycle of the boreal biome. Nat. Commun. 5:4270. https://doi.org/10.1038/ncomms5270.
Zhang, Y., Song, C., Sun, G., Band, L.E., Noormets, A., Zhang, Q., 2015. Understanding moisture stress on light use efficiency across terrestrial ecosystems based on global flux and remote-sensing data. J. Geophys. Res. Biogeosci. 120 (10), 2053–2066.